


Transcriptomic, proteomic, and biochemical analyses reveal a novel neuritogenesis mechanism of *Naja naja* venom α -elapitoxin post binding to TrkA receptor of rat pheochromocytoma cells

Taufikul Islam¹ | Munmi Majumder² | Bhargab Kalita¹ | Atanu Bhattacharjee³ |
Rupak Mukhopadhyay² | Ashis K. Mukherjee¹ 

¹Microbial Biotechnology and Protein Research Laboratory, Department of Molecular Biology and Biotechnology, School of Sciences, Tezpur University, Tezpur, Assam, India

²Cellular, Molecular, and Environmental Biotechnology Laboratory, Department of Molecular Biology and Biotechnology, School of Sciences, Tezpur University, Tezpur, Assam, India

³Department of Biotechnology and Bioinformatics, North Eastern Hill University, Shillong, Meghalaya, India

Correspondence

Ashis K. Mukherjee, Department of Molecular Biology and Biotechnology, School of Sciences, Tezpur University, Tezpur-784028, Assam, India.
Email: akm@tezu.ernet.in

Funding information

Science and Engineering Research Board, Grant/Award Number: SERB/F/9755/2015-2019; Department of Biotechnology, Ministry of Science and Technology, Grant/Award Number: BT/410/NE/U-Excel/2013 and DBT/IC2/Indo-Russia/2014-16/03

Read the Editorial Highlight for this article on page 599.

Abstract

This is the first report showing unique neuritogenesis potency of Indian Cobra *N. naja* venom long-chain α -neurotoxin (Nn- α -elapitoxin-1) exhibiting no sequence similarity to conventional nerve growth factor, by high-affinity binding to its tyrosine kinase A (TrkA) receptor of rat pheochromocytoma (PC-12) cells without requiring low-affinity receptor p⁷⁵NTR. The binding residues between Nn- α -elapitoxin-1 and mammalian TrkA receptor are predicted by in silico analysis. This binding results in a time-dependent internalization of TrkA receptor into the cytoplasm of PC-12 cells. The transcriptomic analysis has demonstrated the differential expression of 445 genes; 38 and 32 genes are up-regulated and down-regulated, respectively in the PC-12 cells post-treatment with Nn- α -elapitoxin-1. Global proteomic analysis in concurrence with transcriptomic data has also demonstrated that in addition to expression of a large number of common intracellular proteins in the control and Nn- α -elapitoxin-1-treated PC-12 cells, the latter cells also showed the expression of uniquely up-regulated and down-regulated intracellular proteins involved in diverse cellular functions. Altogether, the data from transcriptomics, proteomics, and inhibition of downstream signaling pathways by specific inhibitors, and the immunoblot analysis of major regulators of signaling pathways of neuritogenesis unambiguously demonstrate that, similar to mouse 2.5S-nerve growth factor, the activation of mitogen activated protein kinase/extracellular signal-regulated kinase is the major signaling pathway for neuritogenesis by Nn- α -elapitoxin-1. Nonetheless, fibroblast growth factor signaling and heterotrimeric G-protein signaling pathways were found to be uniquely expressed

Abbreviations: BDNF, brain-derived neurotrophic factor; BSA, bovine serum albumin; CV, column volume; DAPI, 4',6-diamidino-2-phenylindole; DMEM, Dulbecco's modified Eagle medium; ELISA, enzyme-linked immunosorbent assay; ERK, extracellular signal-regulated kinase; FBS, fetal bovine serum; FGF, fibroblast growth factor; FITC, fluorescein isothiocyanate; FPLC, Fast protein liquid chromatography; HEK-293, human embryonic kidney 293 cells; HRP, horseradish peroxidase; K_d , equilibrium dissociation constant; KEGG, Kyoto Encyclopedia of Genes and Genomes; L6, immortalized rat skeletal (L6) myoblast cell line; MAPK, microtubule associated protein kinase; MCF-7, Michigan Cancer Foundation-7; MDA-MB-231, triple-negative breast cancer cell line; MS, mass spectrometry; MTT, 3-(4,5-dimethylthiazol-2-yl)-2,5-diphenyl tetrazolium bromide; Mw, molecular weight; nAChR, nicotinic acetylcholine receptors; NCBI, National Center for Biotechnology Information; NGF, nerve growth factor; NPT, normal pressure temperature; NT-3, neurotrophin-3; p⁷⁵NTR, a member of the tumour necrosis factor (TNF) receptor superfamily; PBS, phosphate-buffered saline; PC-12, pheochromocytoma cell line 12; PDB, Protein Data Bank; PI3K, phosphoinositide 3-kinase; PLA₂, phospholipase A2; PLC γ , phospholipase C gamma; PVDF, polyvinylidene fluoride or polyvinylidene difluoride; RDF, radial distribution function; Rg, radius of gyration; RIPA, radioimmunoprecipitation assay buffer; RMSD, root mean square deviation; RMSF, root mean square fluctuation; RP-UHPLC, reversed phase ultrahigh performance liquid chromatography; SASA, solvent accessible surface area; SDS-PAGE, sodium dodecyl sulfate-polyacrylamide gel electrophoresis; TFA, trifluoroacetic acid; TMB/H₂O₂, 3,3',5,5'-tetramethylbenzidine; TNF, tumour necrosis factor; Tris-Cl, Tris (hydroxymethyl) aminomethane (THAM) hydrochloride; Trk, tyrosine kinases.



in Nn- α -elapitoxin-1-treated PC-12 cells and not in mouse 2.5S-nerve growth factor-treated cells. The TrkA binding region of Nn- α -elapitoxin-1 may be developed as a peptide-based drug prototype for the treatment of major central neurodegenerative diseases.

KEYWORDS

Alpha-cobrotoxin, alpha-elapitoxin, Indian Cobra venom, MAPK pathway, nerve growth factor, neuritogenesis, snake venom

1 | INTRODUCTION

The neurotrophins, a diverse class of structurally related proteins, are responsible for apposite development, maintenance, and functioning of the vertebrate nervous system (Hempstead, 2006). Based on structure-function properties, neurotrophins are categorized as: (a) nerve growth factors (NGF), (b) brain-derived neurotrophic factors, and (c) neurotrophin-3 (Park & Poo, 2012). Neurotrophins function via activating two different classes of receptors, the tyrosine kinases (Trk) family of receptor tyrosine kinases and p⁷⁵NTR—a member of the tumour necrosis factor receptor superfamily (Huang & Reichardt, 2001). Neurotrophins activate several cell signaling pathways, including those mediated by Ras and members of the cdc-42/Ras/Rho G protein families, mitogen-activated protein kinase, phosphoinositide-3 kinase, and Jun kinase cascades to induce neuritogenesis in nerve cells (Huang & Reichardt, 2001; Joca, Moreira, & Wegener, 2015). Some recent studies have suggested that neurotrophins may be drug-prototype candidates for therapeutic applications in treating major central neurodegenerative diseases and peripheral neuropathies, such as Alzheimer's and Parkinson's diseases (Chen, Sawa, & Mobley, 2017; Longo & Massa, 2013).

Proteomic analyses have shown that snake venom contains a relatively low proportion of NGF (Chanda, Kalita, Patra, Senevirathne, & Mukherjee, 2018; Kalita, Patra, Das, & Mukherjee, 2018), with a molecular mass ranging from 12.5 to 28 kDa (Trummal et al., 2011). In contrast, three-finger toxins (3FTxs), a major class of non-enzymatic toxins of elapid venoms mostly represented by α -neurotoxins and cytotoxins, have been shown to make up 60% to 74% of Indian Cobra (*Naja naja*) venom (Chanda et al., 2018; Sintiprungrat et al., 2016). The short-chain α -neurotoxins (60–62 amino acid residues) bind to muscle-type nicotinic acetylcholine receptors (nAChRs) to inhibit its action potential (Dutta et al., 2017; Nirthanam & Gwee, 2004), whereas the long-chain α -neurotoxins (66–75 amino acid residues) bind to nAChRs of neuronal receptors to block their function (Alama et al., 2011; Nirthanam & Gwee, 2004). The α -elapitoxin-Dpp2d isolated from black mamba has been characterized and shown to inhibit $\alpha 7$ neuronal nicotinic acetylcholine receptor (nAChR; IC₅₀, 58 ± 24 nM) and muscle-type nAChR (IC₅₀, 114 ± 37 nM) albeit at a concentration of 1 μ M, it did not inhibit the $\alpha 3\beta 2$ and $\alpha 3\beta 4$ nAChR isoforms (Wang et al., 2014). The binding sites for the α -neurotoxins to different cellular receptors have been largely decoded and the astonishing plasticity offered by 3FTxs to fold during the course of

evolution to accommodate the various combinations of functional groups generates target specificities among the different receptors (Lyukmanova, Shenkarev, & Shulepko, 2015). Alpha-neurotoxins have long been used as specific probes to detect and quantify nicotinic ACh receptors (Ben-rong & Ze, 1995), though the binding of α -neurotoxin to the TrkA receptor of nerve cells and the subsequent induction of neurite outgrowth, and the mechanism of neuritogenesis have never been demonstrated.

Interestingly, the present study shows a unique finding that a long-chain α -neurotoxin named Nn- α -elapitoxin-1 purified from Indian Cobra *N. naja* venom functions as a novel neurotrophin-like molecule to induce neurite outgrowth in pheochromocytoma cell line 12 (PC-12) cells by high-affinity binding to the TrkA receptor without requiring p⁷⁵NTR. This study offers an example of a distinct and unique function of a known snake venom component and has made contribution to our advancement in understanding the neuritogenesis mechanism of Cobra venom α -elapitoxin. The TrkA receptor binding region and hot-spot residues of Nn- α -elapitoxin-1 were identified by in silico alanine scanning mutagenesis study. Further, proteomics and transcriptomics analyses of Nn- α -elapitoxin-1-treated PC-12 cells with a comparison to mouse 2.5S-NGF-treated PC-12 cells provide an in-depth understanding of the molecular mechanism of neuritogenesis including activation of intracellular signaling cascades by the Cobra venom toxin under study. This study has pinpointed the differences in the neuritogenesis mechanism between mouse 2.5S-NGF (a conventional mammalian neurotrophin molecule) and Nn- α -elapitoxin-1 and has paved the way for the development of peptide-based neurotrophic drug prototypes in near future.

2 | MATERIALS AND METHODS

The pooled Indian Cobra (*Naja naja*) venom was procured from Calcutta Snake Park, Kolkata, India. The primary antibodies against cell signaling proteins and cell surface receptors were procured from Cell Signaling Technology (CST), Boston. All cell culture reagents including the Dulbecco's modified Eagle's medium (DMEM) media, fetal bovine serum, antibiotics and trypsin-EDTA were obtained from Gibco and Invitrogen. Cell culture accessories and sterile plastic wares were procured from Corning®, Sigma-Aldrich. Radioimmunoprecipitation assay lysis buffer and



recombinant human NTRK1 (TrkA) receptor (protein length 441–596 amino acids) were obtained from Thermo Fisher Scientific. The nerve growth factor 2.5S from murine submaxillary gland, rabbit anti-NGF primary antibody (RRID:AB_477660), rabbit anti-TrkA, anti-TrkB, anti-TrkC, and anti-p⁷⁵NTR primary antibodies were procured from Cell Signaling Technology. The mouse anti-rabbit IgG antibody, horseradish peroxidase (HRP)-conjugate, and rabbit anti-horse IgG HRP-conjugated secondary antibody, fluorescein isothiocyanate (FITC), Thiazolyl Blue Tetrazolium Bromide (for 3-(4,5-dimethylthiazol-2-yl)-2,5-diphenyl tetrazolium bromide assay), and protease inhibitor cocktail were obtained from Sigma-Aldrich. The polyvalent antivenom was purchased from Premium Serum and Vaccines Pvt. Ltd. (Batch no. 012015). Further, the chemical inhibitors of the downstream signaling pathways were bought from Sigma-Aldrich as described in the SI S1.1. The phospholipase A₂ enzyme (NnPLA₂-I) was purified from eastern India *N. naja* venom by the previously described method (Dutta, Gogoi, & Mukherjee, 2015). Details of chemicals/reagent and kits used in the experiments are described in the SI S1.1. The adherent rat PC-12 (RRID:IMSR_CVCL_F659) derived from adrenal gland of *Rattus norvegicus*, a model cell line expressing p140TrkA and p75 receptors to assay nerve growth factor, human breast adenocarcinoma cell lines (Michigan Cancer Foundation-7, MCF-7; RRID:CVCL_0031 and MDA-MB-231; RRID:CVCL_0062) expressing p140TrkA and p75 receptors (Descamps et al., 2001), rat myoblast or myogenic cells (L6; RRID:CVCL_UI07), and human embryonic kidney cell line (HEK-293; RRID:CVCL_0045) were obtained from American Type Culture (ATCC), USA (Perera et al., 2019). The specification sheets provided by ATCC stated the authenticity as well as microbial contamination free cell lines procured from them. The passage number of the cell lines received from ATCC was—(a) PC-12, initial passage number 11; (b) MCF-7, initial passage number 23; (c) MDA-MB-231, initial passage number 16; (d) HEK-293, initial passage number 14; (e) L6, initial passage number 08. During the experiment schedule, each cell line was subjected to 4–5 more passages.

2.1 | Purification of a low molecular mass neurite-inducing (neuritogenesis) protein from *Naja naja* venom

Lyophilized *N. naja* venom (25 mg) in 20 mM Tris-Cl buffer (pH 7.4) was filtered through a 0.2-micron membrane filter, and then fractionated using a HiPrep CM FF 16/10 cation-exchange column previously equilibrated with 20 mM Tris-Cl buffer (pH 7.4) and coupled to an Fast protein liquid chromatography system (AKTA purifier, Wipro GE Health Care). The flow rate was set at 1 ml/min and fraction volume of 1.5 ml was collected. The unbound proteins were eluted from the column by passing one and a half column volume of buffer A and the bound proteins were then eluted with a linear gradient (from 0% to 100%) of 1 M NaCl dissolved in buffer A (buffer B). Elution of proteins was monitored at 280 nm. The fractions were pooled,

desalted by passing through PD-10 column, vacuum dried and then assayed for their ability to induce neurite outgrowth in PC-12 cells (see below).

The fraction showing appreciable neuritogenesis in PC-12 cells was dissolved in 100 µl of solution A (Type-I deionized water containing 0.1% trifluoroacetic acid, TFA) and then subjected to reversed-phase ultrahigh performance chromatography (RP-UHPLC) using an Acclaim 300 C₁₈ (4.6 × 150 mm, 3.0 µm) column equilibrated with solution A. After washing the unbound proteins with solution A, bound proteins were eluted from the column by using a multistep gradient of 5% solvent B (0.1% v/v TFA in 95% v/v acetonitrile) from 0 to 2 min, 5% to 46% solvent B from 2 to 3 min, 46% to 47.1% solvent B from 3 to 15 min, 47.1% to 100% solvent B from 15 to 17 min and at 100% solvent B from 17 to 19 min. The flow rate was adjusted to 0.5 ml/min and fraction volume was 250 µl. Elution of proteins/peptides were monitored at 280 nm and protein content of each peak was determined (Lowry, Rosebrough, Farr, & Randall, 1951). The UHPLC peaks were further screened for neurite inducing bioassay in PC-12 cells (see below).

The apparent molecular mass of the RP-HPLC purified fraction (20 µg) showing neuritogenesis was determined by 12.5% sodium dodecyl sulfate–polyacrylamide gel electrophoresis (SDS-PAGE) under reduced and non-reduced conditions. The gel was stained with 0.1% Coomassie Brilliant Blue R-250 and then destained with methanol/acetic acid/water (40:10:50). Approximate molecular masses of the proteins were determined from a plot of log MW of standards versus. *R_f* values (Mukherjee & Mackessy, 2014).

The molecular mass and purity of the RP-UHPLC purified protein were also determined by MALDI-TOF mass spectrometry using a Bruker Daltonics ULTRAFLEXEXTREME mass spectrometer. Purified protein (~5 µg) in 0.1% TFA was mixed with 1.0 µl of α-cyanosinapinic acid matrix (10 mg/ml) dissolved in 50% (v/v) acetonitrile containing 0.1% (v/v) TFA. The mass of the protein was analyzed in linear analysis mode using an acceleration voltage of 25 kV.

It has been demonstrated that the 3FTxs and NGF form complexes with PLA₂ enzyme of Cobra venom (Dutta, Sinha, Dasgupta, & Mukherjee, 2019). Therefore, to exclude the possibility of co-elution of NGF and PLA₂ along with RP-HPLC purified Nn-α-elapitoxin-1, the immunological cross-reactivity between Nn-α-elapitoxin-1 and rabbit anti-NGF polyclonal antibody/rabbit anti-NnPLA₂-I polyclonal antibody (Dutta et al., 2015) was determined by ELISA (SI S1.2). Furthermore, the PLA₂ activity of RP-HPLC purified protein, if any, was also assayed by Cayman PLA₂ assay kit. The Nn-PLA₂-I (Dutta et al., 2015) was used as a positive control.

2.2 | Mass spectrometric identification of purified protein showing neuritogenesis potency

The reversed-phased purified fraction showing neuritogenesis activity was identified by tandem mass spectrometry analysis of the trypsin digested samples (Patra, Kalita, Chanda, & Mukherjee, 2017). Briefly, 30 µg of the UHPLC-purified protein after reduction and



alkylation with 10 mM dithiothreitol (DTT) 50 mM iodoacetamide (in the dark), respectively, was incubated with sequencing-grade trypsin (50 ng/μl in 25 mM ammonium bicarbonate containing 10% acetonitrile) for 18 hr at 37°C. The digested peptides were desalted and concentrated using ZipTip (Millipore), re-suspended in 20 μl of 0.1% (v/v) formic acid in 2% acetonitrile, and then 1 μl sample was subjected to nano-UHPLC-MS/mass spectrometry (MS) analysis. ESI (nano-spray) was used as the ion source, fragmentation mode used was collision-induced dissociation (y and b ions), FT-ICR/Orbitrap was used as MS scan mode and MS/MS scan in the range from 500 to 2000 m/z was linear ion trap. Doubly or triply-charged ions were selected for collision-induced dissociation (CID) MS/MS analysis.

For analysis of MS/MS data, carbamidomethylation of cysteine residues and oxidation of methionine residues were selected for fixed and variable modifications, respectively. The percent mass error tolerance and fragment mass error tolerance were set to 12 ppm and 0.8 Da, respectively. The data were searched against the UniProt and Swiss-Prot database (non-redundant database with reviewed proteins) for Elapidae venom from National Center for Biotechnology Information (NCBI) and the data were analyzed with Proteome 1.4 Discoverer software.

The multiple sequence alignment of the tryptic peptides identified by LC-MS/MS analysis with other homologous protein sequences deposited NCBI database was performed using Clustal Omega. The distinct peptide sequences obtained were subjected to Standard Protein BLAST (<https://blast.ncbi.nlm.nih.gov/Blast.cgi?PAGE=Proteins>) to retrieve similar sequences in the NCBI database. Using the obtained sequences from NCBI, Multiple Sequence Alignment (MSA) of the identified distinct peptides was performed using the Clustal Omega (<https://www.ebi.ac.uk/Tools/msa/clustalo/>) online server. Similarly, protein sequences of NGF from various snake venoms were downloaded from the NCBI database and MSA was performed using the Clustal Omega software as mention above.

2.3 | Assay of neurite outgrowth, cell viability, cellular morphology, and DNA fragmentation in PC-12 cells by Nn-α-elapitoxin-1

The biological activity (in terms of induction of neurite outgrowth) of Nn-α-elapitoxin-1 was determined in PC-12 cells (Rubenstein, Carp, & Callahan, 1984) because this cell exhibits several neuronal properties including morphological differentiation, electrophysiological responsiveness, and neurotransmitter synthesis (Rubenstein et al., 1984). Therefore, this cell line is routinely used by scientists to characterize the neurotrophins. Briefly, PC-12 cells (0.5×10^5) were grown in six-well cell culture plate in DMEM containing 10% fetal bovine serum at 37°C, 5% CO₂ and allowed to adhere for 24 hr to the substratum of the culture plate. On the next day, old medium was replaced with fresh DMEM containing RP-HPLC purified (25–100 ng/ml) Nn-α-elapitoxin-1 or 100 ng/ml of mouse 2.5S-NGF (positive control) or DMEM (control). After incubation for 14 days the neurite outgrowth from PC-12 cells was visualized under a light

microscope (Olympus IX 83) and photographed at 40x magnification using a sCMOS camera. The length of neurite (in μm) emerged from PC-12 cells was measured using MOTIC IMAGE PLUS 3.0 software. The change in cellular morphology of treated cells, if any, was determined by observing the cells (treated as well as control) under a phase-contrast microscope (Olympus IX 83) at 40X magnification.

For cell viability assay, PC-12, MCF-7, MDM-MB-231, L6 and HEK-293 cells (0.5×10^5) were grown in 96-well plate as described above. Then, 200 ng/ml of Nn-α-elapitoxin-1/mouse 2.5S-NGF/1X phosphate-buffered saline (PBS) (control) was added to wells in triplicate and cell viability was assessed after 72 hr of inoculation by 3-(4,5-dimethylthiazol-2-yl)-2,5-diphenyl tetrazolium bromide-based method (Riss et al., 2016). The Nn-α-elapitoxin-1/mouse 2.5S-NGF-induce cytotoxicity, if any, was expressed as percent viability as determined from a standard curve of control cells (Dutta et al., 2015).

For the DNA fragmentation assay, PC-12 cells (1×10^4 cells/ml) were seeded in T-25 cultured flasks and incubated with 100 ng/ml of Nn-α-elapitoxin-1/1X PBS (control) for 14 days at 37°C, 5% CO₂. The old medium at an interval of 7 days was replaced with fresh DMEM containing Nn-α-elapitoxin-1. The adherent cells post 14 days of incubation were harvested by trypsinization, combined with floated (non-adherent) cells, and washed with 1X PBS. The genomic DNA was isolated from the cells using a GeneJET Genomic DNA Purification Kit (ThermoFisher Scientific), and the concentration and purity of DNA was estimated at 260 nm, and 260/280 nm using a spectrophotometer (NanoDrop 2000; Thermo Scientific). Then 150 ng of DNA from the treated as well as control cells was separated by electrophoresis on 0.8% agarose gel. The DNA was visualized at 260 nm by adding ethidium bromide and the gel was photographed with a CCD camera attached to an image analyzer (ChemiDoc™ XRS + System; BioRad).

2.4 | Determination of binding of Nn-α-elapitoxin-1 to mammalian cells expressing TrkA and p⁷⁵NTR receptors

The mammalian cells expressing TrkA receptors such as PC-12, MCF-7, and MDM-MB-231 (0.5×10^5) (Descamps et al., 2001) were grown in 96 well cell culture plate in DMEM and then anti-TrkA, TrkB, TrkC or p⁷⁵NTR primary antibody (1:1,000 in DMEM) or 1X PBS (control) was added to each well. The cells that did not express TrkA receptor such as HEK-293 and L6 were used as negative controls. After incubation with antibodies/1X PBS (control) for 1 hr at 37°C, 5% CO₂, the cells were washed with 1x PBS and then Nn-α-elapitoxin-1 (100 ng/ml, 12.79 nM)/mouse 2.5S NGF(100 ng/ml,3.77 nM, positive control) was added to each well and incubated for 2 hr at 37°C, 5% CO₂. The cells were washed with 1X PBS and the binding of Nn-α-elapitoxin-1 to PC-12 cells was determined by ELISA using anti-Nn-α-elapitoxin-1 specific equine antibody (1:1,000)/rabbit anti-NGF antibody (for determination of binding of mouse 2.5S-NGF) and rabbit anti-horse IgG



conjugated with horseradish peroxidase (HRP)/mouse anti-rabbit IgG HRP conjugate (1:2000) as the secondary antibody. The isolation procedure of anti-Nn- α -elapitoxin-1 antibodies from commercial polyvalent antivenom is described in SI S1.3. Similarly, rabbit anti-NGF antibody and mouse anti-rabbit IgG HRP-conjugate antibody were used as primary and secondary antibodies for the detection of mouse 2.5S-NGF binding to PC-12 cells. The binding of Nn- α -elapitoxin-1 to 1X PBS-treated cells (control)/mouse 2.5S NGF was considered as base value (100% binding) and other values (binding in presence of anti-receptor antibodies) were compared with that.

In a different set of experiments, Nn- α -elapitoxin-1 and mouse 2.5S-NGF were conjugated with FITC following the instructions of the manufacturer with slight modifications (for detail protocol see SI S1.4). The PC-12, MCF-7, and MDA-MB-231 cells (10×10^4 cells per well) as well as HEK-293, and L6 cells (negative control) were incubated with FITC-Nn- α -elapitoxin-1 or mouse 2.5S-NGF conjugate (1 μ g/ml protein content equivalent to \sim 121.91 nM) for 240 min at 37°C, 5% CO₂. The washed cells were stained with 4',6-diamidino-2-phenylindole for 3 min, washed with PBS, pH 7.4 and then fixed in 4% formaldehyde-PBS solution (pH 7.2) for 15 min at room temperature (\sim 23 °C). After fixation, the cells were washed with 1X PBS, pH 7.4, mounted on a cover slip and observed under a fluorescent microscopy (Olympus IX 83) at 40 \times magnification. The green and blue fluorescence filters were used for FITC and 4',6-diamidino-2-phenylindole, respectively and the fluorescence signal was captured by a CCD camera.

2.5 | Binding of Nn- α -elapitoxin-1 to recombinant human TrkA receptor

The spectrofluorometric interaction between Nn- α -elapitoxin-1 and water soluble cytoplasmic domain (amino acids 441–796) of TrkA receptor was determined as stated previously (Dutta et al., 2019). Briefly, graded concentrations (0.625 pM to 0.625 nM) of Nn- α -elapitoxin-1/mouse 2.5S-NGF (positive control)/bovine serum albumin (BSA) (negative control) in a total volume of 100 μ l were incubated with a fixed concentration of recombinant TrkA receptor (25 nM) in Nunc™ F96 MicroWell™ Black Polystyrene Plate (Thermo Fisher Scientific). Excitation of the proteins mixture was done at 280 nm with a monochromatic light source maintaining a slit width of 12 nm and the emission spectrum was recorded from 300 to 500 nm in a multimode microplate Reader (Varioskan LUX; Thermo Fisher Scientific). The emission spectrum of the individual protein (TrkA receptor, mouse 2.5S-NGF, and Nn- α -elapitoxin-1) was compared with the fluorescence spectra (λ max) of the mouse 2.5S-NGF/Nn- α -elapitoxin-1 interacting with the TrkA receptor.

In another set of experiments, the affinity for binding of Nn- α -elapitoxin-1 and its binding partner mouse 2.5S-NGF toward cytoplasmic domain of recombinant TrkA receptor was determined by competitive ELISA. Briefly, 30 nM of recombinant cytosolic domain of TrkA (in 100 μ l coating buffer) was coated on to ELISA plate and

incubated overnight at 4°C. Next day, after blocking the wells with fat-free milk and washing with 1X PBS, mouse 2.5S-NGF and Nn- α -elapitoxin-1 mixed in different molar ratios (1:0, 1:0.25, 1:0.50, 1:0.75, 1:1, 0:1) were added to the wells of the ELISA plate and incubated for 4 hr at room temperature (\sim 23 °C). Thereafter, the wells were washed with 1X PBS, incubated with rabbit anti-NGF antibody (1:1,000) in 100 μ l PBS for 2 hr at room temperature (\sim 23 °C) followed by incubation with mouse anti-rabbit IgG HRP conjugate (1:2000) for 2 hr at room temperature (\sim 23 °C). After washing the wells, 100 μ l of substrate (1 \times 3,3',5,5'-tetramethylbenzidine/H₂O₂) was added to each well and the reaction could proceed in the dark for 30 min at room temperature (\sim 23 °C). The reaction was stopped by adding 50 μ l of 2M H₂SO₄ to each well and the color developed was measured at 492 nm against blanks in a microplate reader.

2.6 | Effect of anti-TrkA, TrkB, TrkC, and p⁷⁵NTR antibodies and chemical inhibitor of TrkA receptor on Nn- α -elapitoxin-1-induced neuritogenesis in PC-12 cells

PC-12 cells (0.5×10^5 cells/ml) were cultured in six-well plates in DMEM at 37°C in 5% CO₂ for 24 hr. The cells were washed with serum-free DMEM and allowed to grow for an additional 24 hr in the same medium. Thereafter, the medium was replaced with DMEM containing 10% horse serum and cells were allowed to grow for 24 hr in the above conditions. The neurite outgrowth from PC-12 cells was observed under two different conditions. In condition A, the cells were treated with anti-TrkA/TrkB/TrkC/p⁷⁵NTR antibodies (1:1,000), or anti-TrkA, TrkB, TrkC, and p⁷⁵NTR (1:1:1:1) antibodies, or 100 nM K252a (chemical inhibitor of TrkA receptor), or DMEM (control). After incubation for 1 hr at 37°C, 5% CO₂, 100 ng/ml of Nn- α -elapitoxin-1 or mouse 2.5S NGF (positive control) was added to each well and incubated for 14 days. For control wells, DMEM was added. After 14 days of growth, neurite outgrowth from PC-12 cells was observed under a light microscope (Olympus IX 83) and neurite length was measured as stated above.

In a separate set of experiments (condition B), the PC-12 cells (0.5×10^5 cells/ml) were incubated with 100 ng/ml of Nn- α -elapitoxin-1 for 1 hr at 37°C, 5% CO₂ and then treated with anti-TrkA/TrkB/TrkC/p⁷⁵NTR antibody or DMEM (control) as stated above. After 14 days of growth of PC-12 cells, neurite outgrowth was visualized, and neurite length was measured.

2.7 | Computational (in-silico) analysis to determine the binding region of Nn- α -elapitoxin-1 with mammalian TrkA receptor

To further understand the interaction between Nn- α -elapitoxin-1 and mammalian TrkA receptor as well as to determine the TrkA receptor binding region of Nn- α -elapitoxin-1, the in silico analysis was performed.



2.7.1 | Homology modeling of TrkA receptor and its docking complexes

The 3D structure of rat TrkA receptor was not available in Protein Data Bank; therefore, its structure was deciphered using comparative homology modeling by Swiss-Model server (Schwede, Kopp, Guex, & Peitsch, 2003). The human TrkA receptor was selected as a template on the basis of the amino acid sequence similarity with the query rat TrkA sequence (uniprot ID: P35739) performed by BLAST search from PDB. The spatial structure of human TrkA receptor has been illustrated by NMR (PDB ID: 1HE7). The refinement of the modeled rat TrkA structure was performed using Swiss PDB Viewer (Guex & Peitsch, 1997) by energy minimization using GROMOS96 43B1 force field. ERRAT score, PROCHECK, Profiles-3D were analyzed through Structural Analysis and Verification server (SAVES) version 4 (<https://services.mbi.ucla.edu/SAVES/>). The ProSA-web server (<https://prosa.services.came.sbg.ac.at/prosa.php>) was used for calculation of knowledge-based energy and Z-score (Wiederstein & Sippl, 2007) for the structural validation of the modeled TrkA.

On the basis of LC-MS/MS analysis result, the PDB structure with ID 1CTX was selected for long-chain α -neurotoxin, whereas 1BET is the active form of mouse NGF. The modeled rat TrkA receptor complex structures formed with long-chain α -neurotoxin from Cobra venom (PDB ID: 1CTX) as well as mouse NGF (PDB ID:1BET) were docked using PATCHDOCK ([http://bioinfo3d.cs.tau.ac.il/Patch Dock/](http://bioinfo3d.cs.tau.ac.il/PatchDock/)) web server employing geometry-based docking algorithm (Duhovny, Nussinov, & Wolfson, 2002) to determine the optimum candidate solutions. The root mean square deviation (RMSD) clustering was used to remove redundant solutions. The geometric fit as well as atomic desolvation energy were considered for scoring the docked structures keeping the default RMSD value of 4 Å for clustering solutions (Zhang, Vasmatzis, Cornette, & DeLisi, 1997).

2.7.2 | Molecular dynamics simulations and computational analysis to determine the interaction between Nn- α -elapitoxin-1 and mammalian TrkA receptor

The best resulting complexes from the docking study (TrkA-1CTX and TrkA-1BET) were further evaluated for interface residues using PDBSUM (Laskowski, 2001) with a contact distance of less than 6 Å (Kruger & Gohlke, 2010). Furthermore, potential hot-spot residues were identified by alanine scanning mutagenesis using Drugscore PPI server (Ofra & Rost, 2003). A residue is considered as a hot-spot if mutation of that particular residue to alanine results in a significant binding free energy change ($\Delta G \geq 2$ kcal/mol) (Li, Keskin, Ma, Nussinov, & Liang, 2004).

Both the systems (TrkA-1BET and TrkA-1CTX) were simulated using the topology file generated by GROMOS96 43a1 force field as starting structures for 30 ns time scale of MD simulation. The stability of both the systems was analyzed by considering the RMSD of C-alpha atoms of TrkA receptor. The preparation of each system

involves explicit solvation in a cubical box with simple point charge (SPC216) water molecules at 10 Å from the box edges followed by neutralization of the system by addition of Na⁺ ions (8 Na⁺ ions in TrkA_1BET and 6 Na⁺ ions in TrkA_1CTX). The solved systems were further energy minimized using steepest descent algorithm until maximum force reached <1,000.0 kJ mol⁻¹ nm⁻¹. Subsequent unrestrained production MD was run for 30 ns with a time step of 500 ps, semi-isotropic pressure of 1 bar in isothermal-isobaric (normal pressure temperature) condition. The analysis was carried out using Linear Constraint Solver (LINC) algorithm (Hess, Bekker, Berendsen, & Fraaije, 1997) and the electrostatic interactions were calculated using Particle Mesh Ewald (PME) (Darden, York, & Pedersen, 1993). A constant pressure of 1 bar and temperature of 300 K were maintained by coupling the system using Parrinello-Rahman (Parrinello & Rahman, 1980) and modified Berendsen thermostat (Hess et al., 1997) algorithms, respectively, with a relaxation time of 0.1 ps. All the simulations [RMSD plot versus. time (ps), root mean square fluctuation plot versus. residue number, number of intermolecular hydrogen bonds versus. time (ps), radius of gyration (R_g) plot versus. time (ps), total solvent accessible surface area (nm²) versus. time (ps), distance (nm) versus. time (ps), radial distribution function (RDF) plot versus. time (ps)] were performed using GROMACS versus. 4.6.5 package (Hess, 2008). The graphs were plotted using Xm grace plotting tool (<http://plasma-gate.weizmann.ac.il/Grace/>).

2.8 | Effect of Nn- α -elapitoxin-1 on mobility of PC-12 cell-surface TrkA receptor

PC-12 cells were adhered onto cover slips (submerged in 6-well cell culture plates) for 24 hr at 37°C in a 5% CO₂ incubator. Next day, the old DMEM was replaced with fresh media containing 100 ng/ml of Nn- α -elapitoxin-1 (12.8 nM)/mouse 2.5S-NGF (3.78 nM)/1X PBS (untreated control) and the cells were grown for different time intervals (0 to 360 min). After washing with 1X PBS for three times the cells were fixed with 4% paraformaldehyde (in 1X PBS) for 30 min, then washed in 1X PBS, followed by blocking with 10% horse serum containing 1% (w/v) BSA. Subsequently, the cells were permeabilized by treating with 0.5% Triton X-100 in 1X PBS for 1 hr at room temperature (~23 °C). The slides were then incubated for 3 hr with rabbit anti-TrkA primary antibody (1:150) in PBS (containing 1% BSA, 0.5% triton X-100) at 4°C for 3 hr. The cells were washed and incubated with Alexa Fluor 488 dye bound to goat anti-rabbit secondary antibody (ThermoFisher Scientific) for 1 hr at room temperature (~23 °C) in dark. The cover slips were washed with 1X PBS, mounted using ProLong Antifade Kit (ThermoFisher Scientific) according to manufacturer's instructions, and the cells were observed under a fluorescence microscope (Olympus IX 83) using a green filter (~525 nm emission) (Melan & Sluder, 1992) and photographed with a CCD camera.

In another set of experiments, the PC-12 cells (0.5×10^5) were grown in a 96-well cell culture plate at 37°C in a 5% CO₂ incubator for 24 hr. The old media was replaced with fresh media containing

10% fetal bovine serum (in PBS-T containing 1% BSA). After washing the cells three times, they were treated with Nn- α -elapitoxin-1 (12.8 nM)/mouse 2.5S-NGF (3.78 nM)/1X PBS and were incubated for 0 to 360 min at 37°C, 5% CO₂, followed by washing of the cells with PBS-T (three times for 10 min each). Next, rabbit anti-TrkA primary antibody (1:1,000) was added, incubated for 3 hr at 37°C, 5% CO₂, and the cells were washed with PBS-T. The TrkA receptor bound primary antibodies were detected by incubating with Alexa Fluor™ 568 dye labeled secondary anti-rabbit antibody raised in goat (ThermoFisher Scientific) for 1 hr at 37°C in dark. The fluorescence intensity was determined by excitation at 568 nm ($\lambda_{\text{ex}} = 568 \text{ nm}$) and emission spectra were recorded at 600 nm ($\lambda_{\text{em}} = 600 \text{ nm}$) in a fluorescence microplate reader (Varioskan LUX; Thermo Fisher Scientific). The fluorescence intensity of untreated (control) cells at each time point was considered as base value (100%) and fluorescence intensity of treated cells at that time point was compared with that.

2.9 | Transcriptomic analysis of PC-12 cells post treatment with Nn- α -elapitoxin-1 and mouse 2.5S-NGF

The PC-12 cells were grown in aseptic condition in DMEM media containing 10% fetal bovine serum and incubated at 37°C in 5% CO₂ and allowed to adhere to the substratum. Next day, the cells were treated with 100 ng/ml of Nn- α -elapitoxin-1 and mouse 2.5S-NGF (positive control) and allowed to grow for 14 days under the above conditions. The adherent cells were then harvested, washed three times with 1X PBS, and centrifuging at 250 g for 10 min at 4°C, the cell pellet was kept in RNeasy™ stabilization solution (Thermo Fisher scientific).

After including treatment with DNase, the total RNA was extracted from the cell pellets using the miRNeasy Mini Kit (Qiagen). The quality of the RNA was checked by RNA 6,000 Nano (Agilent Technologies) and quantification was done using by Qubit. All the samples showing RNA integrity numbers (RINs) greater than 7.0 were considered for RNA shearing (0.1–4 μg of RNA). The RNA obtained for each sample was converted to cDNA using MMLV reverse transcriptase (Illumina) and cleaned up by using AM pure beads. The cDNA was subjected to end repair, adenylation of 3' ends, and adapter ligation (for multiplexing). The cDNA library quality and size distribution were checked using a Bio analyzer (Agilent Technologies). To the adenylated fragments, ligation of adapters was performed that ligated multiple indexing adapters to the ends of DNA fragments. Each adapter catalogue had different index sequences and the library fragment sizes were between 200 and 250 bp that was cleaned up using AM pure beads. The transcriptome library obtained was quantified by Qubit and quality check was completed using Agilent DNA 7,500 kit. A normalized transcriptome sample of 4 pmol was considered and sequenced using Illumina's NovoSeq 6,000 (Illumina) (Kapranov, Willingham, & Gingeras, 2007; Tuch et al., 2010).

The raw data obtained from the sequencing was determined for quality using FastQC (Andrews, 2010) through which the adapter sequences were also identified and trimmed using TrimGalore (Krueger et al., 2015). The parameters adopted were “-q 30” and “--retain-unpaired.” Then, sequence indexing of the obtained data was performed by corroborating the latest version of *Rattus norvegicus* (Norway rat) (Rnor_6.0) genome deposited at NCBI genome database (accession No. GCF_000001895.5) using HISAT2 index building binary algorithm (Kim, Langmead, & Salzberg, 2015). The previously created index was taken as input and sequence alignment was performed by considering other parameters such as “-q”, “--mm”, and “--dta” with HISAT2. Furthermore, refinement of the aligned sequences and transcript assembly was carried out using samtools (Li et al., 2009) in order to obtain sorted binary alignments for the transcript assembly. In addition, identification of novel transcripts, assembly of the merged transcript, and quantification- all were ensured using StringTie (Pertea et al., 2015). After proper assembly and quantification of transcripts, ballgown was used for the exploratory analysis and statistical modeling (Pertea et al., 2016). For differential expression analysis, a function within the software package calculated the fold change between conditions, along with the P and q values for differential expression. Moreover each transcript that mapped to a gene locus was further annotated for its gene name/gene symbol/orthologue, family/subfamily and protein class to denote its ontology analysis using PANTHER14.1 (<http://www.pantherdb.org>).

The correlation between the data obtained from transcriptomics and functional proteomics analyses (see below) was conducted by converting the gene list/accession number obtained from transcriptomic and functional proteomics data into pathways elicited after treatment of PC-12 cells with Nn- α -elapitoxin-1 by gene ontology analysis (PANTHER14.1). The Kyoto Encyclopedia of Genes and Genomes server shows involvement of 125 genes (Kyoto Encyclopedia of Genes and Genomes pathway entry: rno04722) of *Rattus norvegicus* in the TrkA receptor mediated neuritogenesis process. The accession numbers of these 125 genes were used to construct the neuritogenesis pathways in *Rattus norvegicus* by gene ontology analysis using PANTHER14.1 online server.

2.10 | Comparison of differential expression of intracellular proteins in Nn- α -elapitoxin-1 and mouse 2.5S-NGF-treated PC-12 cells by quantitative tandem mass spectrometry analysis

The PC-12 cells (0.5×10^7) incubated with DMEM (control) or treated with 100 ng/ml of Nn- α -elapitoxin-1/mouse 2.5S-NGF were grown for 14 days at 37°C, 5% CO₂. The adherent cells were then harvested using trypsin-EDTA, washed three times with 1X PBS, and centrifuged at 250 g for 10 min at 4°C. The cells were lysed with 200 μl radioimmunoprecipitation assay lysis buffer containing cocktail of protease inhibitors and then centrifuged at 14,000 g for 15 min at 4°C to isolate the intracellular proteins present in the supernatant.



For LC-MS/MS protein identification and quantitation, 150 µg intracellular proteins from PC-12 cells treated with Nn-α-elapitoxin-1, and mouse 2.5S-NGF (positive control)/PBS (control) after reduction and alkylation were digested with trypsin at enzyme: substrate ratio of 1:30 for 16 hr at 37°C, using the 'In-Solution Tryptic Digestion and Guanidination Kit' (Thermo Fisher Scientific) following the manufacturer's protocol (Kalita, Patra, & Mukherjee, 2017). The tryptic peptides were analyzed by mass spectrometry and identified proteins were quantitated by label-free quantitative proteomic analysis (see below). Each experiment was run in triplicate to assure the reproducibility.

The separation of the in-solution trypsin-digested peptide fragments were performed on an Agilent 1,200 HPLC system integrated to an LTQ Orbitrap Discovery hybrid mass spectrometer (Thermo Fisher Scientific) via a Nanomate Triversa (Advion BioSciences) (Dutta et al., 2017; Kalita et al., 2017). For the MS scan mode, FT-ICR/Orbitrap was used and a linear ion trap mode from m/z 500 to 2000 was scanned for the MS/MS scan (Dutta et al., 2017; Kalita et al., 2017). The doubly or triply-charged ions were selected for collision-induced dissociation (CID)-MS/MS analysis. The signal-noise ratio was kept >2 when selecting the precursors for MS/MS data acquisition.

All the raw MS/MS data were searched and analyzed using Proteome Discoverer 3.1 software where carbamidomethylation of cysteine residues and oxidation of methionine residues were selected for variable modifications (Chapeaurouge et al., 2015). The percent mass error tolerance was set at 10 ppm and the fragment mass error tolerance was 0.8 Da, and up to three missed cleavages were allowed (Dutta et al., 2017; Kalita et al., 2017; Mukherjee, Kalita, & Mackessy, 2016; Mukherjee & Mackessy, 2014). The LC-MS/MS data of the total intracellular proteins were searched in the NCBI (non-redundant database with reviewed proteins) database against *Rattus norvegicus* protein entries (taxid: 151,655). Contamination in the identification process was nullified by searching and identification of 115 proteins from the contamination database (<ftp://ftp.thegpm.org/fasta/cRAP/crap.fasta>). The redundant peptides (peptides that are present in more than one protein entry) were manually removed from the dataset and the following protein/peptide identification criteria were considered to unambiguously identify proteins: (a) the false discovery rate (FDR) was kept at 0.1% and (b) presence of at least one unique peptide in identified protein.

The change in expression level of intracellular proteins in PC-12 cells grown in the presence of exogenously added Nn-α-elapitoxin-1/mouse 2.5S-NGF in culture media was determined by MS-based label-free proteomics analysis (Mukherjee et al., 2016). The mean spectral count of a protein was normalized by dividing the summed spectra of the identified protein by the number of peptides generated from it (Equation. 1).

$$\text{Mean spectral count of a protein X} = \frac{\text{Total spectral count of X}}{\text{Total number of peptides of X}} \quad (1)$$

Similarly, Equation (2) represents the fold change in expression of protein X, which is denoted as follows: Fold change in mean spectral count =

$$= \frac{\text{Mean spectral count of protein X in presence of mouse 2.5S-NGF or Nn-}\alpha\text{-elapitoxin-1}}{\text{Mean spectral count of protein X in control}} \quad (2)$$

2.11 | Immunoblot analysis to study the expression of cell signaling proteins in Nn-α-elapitoxin-1-treated PC-12 cells

Intracellular proteins from the control as well as Nn-α-elapitoxin-1 treated PC-12 cells were prepared as described above. Forty microgram intracellular proteins were separated by 12.5% of SDS-PAGE and electrophoretically transferred to an iBlot™ polyvinylidene fluoride membrane using a semidry blotter system (TE 77 PWR; Amersham Bioscience). The non-specific sites of polyvinylidene fluoride membrane were blocked by incubating the membrane with 5% BSA (in TBS-T blocking solution containing 0.1% Tween-20) overnight followed by its washing for three times with wash buffer (20 mM Tris buffer saline, pH 7.4 containing 0.1% Tween-20, TBST). The membranes were then incubated with primary antibodies (1:750) against p38, phospho p38, extracellular signal-regulated kinase (Erk) ½, phospho Erk ½, JNK, phospho-JNK, BCL2, NF-κβ, phospho- NF-κβ, BAX, CREB, Phospho-CREB, or β-actin (internal standard) proteins for 1 hr at room temperature (~23 °C). Next, the blots were washed three times with TBS-T, and then incubated with horseradish peroxidase-conjugated mouse anti-rabbit secondary antibodies (1:3,000) for 1 hr at room temperature (~23 °C). After washing with TBS-T, western blots were developed with Clarity™ Max Western ECL Substrate (Bio-Rad Laboratories). The signal was recorded with a CCD camera and analyzed through Quantity Image Lab Software (ChemIDOC Imaging System; BioRad). The experiment was repeated three times to assure the reproducibility. ImageJ 1.8 version software was used for densitometry scanning of the blot. Normalization of the band intensity was done by comparing with β-actin and fold change in protein expression was calculated as follows:

$$\text{Fold change in protein expression} = \frac{\text{normalized band intensity of treated cell}}{\text{normalized band intensity of control cell}} \quad (3)$$

2.12 | Assay of neuritogenesis potency of Nn-α-elapitoxin-1 in presence of synthetic inhibitors of TrkA receptor signaling pathways

2.0×10^4 PC-12 cells (in 24-well plate) were grown in DMEM media at 37°C/5% CO₂. After 24 hr, old media was replaced with fresh media containing specific inhibitors: U0126 (10 µM) (MEPK -Erk 1 and Erk 2 inhibitor), PD98059 (10 µM) (MEPK -high of Erk 1 and low Erk 2 inhibitor), SB203580 (10 µM) (p38 inhibitor), G06976 (3 µM) (PKC inhibitor), LY294002 (10 µM) (Akt inhibitor), H: 89 (10 µM) (PKA inhibitor), SP600125 (10 µM) (JNK inhibitor), 1X PBS (control), and the cells were incubated at 37°C/5% CO₂ for 30 min. Then, 100 ng/ml of Nn-α-elapitoxin-1 (test sample)/mouse 2.5S-NGF (positive control)/1X PBS (control) was added to the cells, and after incubating for 14 days, the neurite outgrowth from PC-12 cells was visualized under a light microscope (Olympus IX 83) and photographed at 40x magnification. The % cell transformed was measured using MOTIC IMAGE PLUS 3.0 software.



2.13 | Statistical analysis of data and study design

For all the statistical analysis of data, except for transcriptomic analysis of gene expression, Sigma Plot 11.0 for Windows (version 10.0) software was used. For exploratory analysis to determine the differential expression of transcripts (the p and q values) as well as statistical modeling of transcripts in order to calculate the fold change between the two conditions, the ballgown software was used. Data normalization for the calculation of P and Q values and to adjust for library size when doing differential expression testing in transcriptomics analysis was done using the ballgown software package. For proteomic analysis of data, Proteome Discoverer 3.1 software was used. All experiments contained a minimum of three replicates ($n = 3$). Results are depicted as mean, \pm standard deviation (SD) of the means are represented by the error bars. The significance of difference between means of two test samples as well as means of test sample and control was determined using Student's t test. A value of $p \leq .05$ was considered statistically significant. No test for outliers was conducted and no data point was excluded. The transcriptomics, proteomics, and immunoblot experiments were conducted in a blinded manner; however, for other experiments the researchers were not blinded to the experimental conditions.

2.14 | Ethical approval

No institutional or ethical approval was needed for this study.

3 | RESULTS

3.1 | Purification of PC-12 cells neurite-inducing proteins from *N. naja* venom

The cation-exchange fractionation of *N. naja* venom resulted in its separation into seven protein peaks, designated as NnCM1 to NnCM7 (Figure 1a). Although the control cells post 14 days of incubation showed some differentiation, but marginal neurite outgrowth was observed. Nevertheless, the NnCM3 and NnCM4 fractions with a protein yield of 0.62 and 5.86 mg, respectively showed significant neurite-inducing property in PC-12 cells (Figure 1b). Because of better neuritogenesis potency of NnCM3 (quantitative data not shown), this fraction was selected for further studies. The RP-UHPLC fractionation of NnCM3 yielded three peaks (NnCM3RP1 to NnCM3RP3) (Figure 1c). All the three peaks demonstrated significant neurite outgrowth in PC-12 cells; however, the NnCM3RP2 fraction was selected for further study (see the reason below). Protein yield of NnCM3RP1, NnCM3RP2, and NnCM3RP3 was 0.4, 1.12, and 1.01%, respectively of the total *N. naja* venom protein.

The treatment of PC-12 cells with reversed-phase purified fractions (0.1 $\mu\text{g/ml}$ equivalent to 0.012 μM) and mouse 2.5S-NGF (0.1 $\mu\text{g/ml}$, 0.003 μM) for 14 days resulted in more neurite-bearing cells, compared to the control PC-12 cells (Figure S1). Nevertheless,

approximately 10–12 days were found to be necessary for the tested neurotrophins to induce visible neurite outgrowth from PC-12 cells (data not shown). All the three RP-UHPLC purified proteins induced significant neurite outgrowth in PC-12 cells, although to a significantly different extent ($p < .05$) (Figure 1d, Figure S1). The neurite-inducing potency (percentage of PC-12 cells showing neurite outgrowth and length of neurite) of NnCM3RP2 and NnCM3RP3 fractions surpassed the same potency exhibited by NnCM3RP1 and mouse 2.5S-NGF (Figure 1d). In contrast to NnCM3RP2, however, the NnCM3RP3 fraction demonstrated an altered cellular morphology of the PC-12 cells, such as enlargement of cell volume with extensive plasma membrane blebbing (Figure S1). Therefore, this fraction was not considered for further characterization. Moreover because of lower protein yield, NnCM3RP1 fraction was also excluded from further investigation. Therefore, the NnCM3RP2 fraction was selected for further study. This fraction did not alter cellular morphology, or the viability of PC-12 cells post 14 days of growth (Figure S1).

The 12% SDS-PAGE analysis of 20 μg of NnCM3RP2 protein under reduced and non-reduced conditions displayed a single band of ~ 9.8 kDa suggesting that it was a monomeric protein (Figure S2). By MALDI-TOF-MS analysis, the NnCM3RP2 fraction showed a protonated molecular ion [MH^+] at m/z 7,813.13 Da and a lower-intensity, doubly-charged [MH^{2+}] peak at m/z 3,904.22 (Figure 1e), thus confirming the purity of the preparation.

The NnCM3RP2 fraction did not show immunological cross-reactivity with anti-NGF antibody, whereas mouse 2.5S-NGF (positive control) was well recognized by anti-NGF antibody (Figure S3). This result demonstrates that the NnCM3RP2 fraction was not contaminated with NGF from *N. naja* venom. Furthermore, NnCM3RP2 fraction at a concentration of 10 $\mu\text{g/ml}$ did not demonstrate PLA_2 activity, as assayed by enzymatic analysis or recognized by anti-Nn- PLA_2 -I antibody by ELISA (data not shown), indicating that the protein preparation was free from venom PLA_2 and NGF contaminations.

The NnCM3RP2 fraction dose-dependently enhanced the neurite outgrowth from the treated PC-12 cells (Figure S4). At the lowest tested dose of 25 ng/ml (~ 2.4 nM), the NnCM3RP2 fraction was found to induce neurite outgrowth from PC-12 cells (Figure S4). The time-dependent (kinetics) analysis showed that neurites appeared from the PC-12 cells approximately 11 days post-treatment with NnCM3RP2 (data not shown). Furthermore, NnCM3RP2 at a dose of 200 nM did not show cytotoxicity against mammalian cells (Figure S5). Moreover Nn- α -elapitoxin-1 at a concentration of 12.84 μM did not induce the fragmentation of genomic DNA in PC-12 cells, suggesting that it lacks pro-apoptotic activity (Figure S6).

3.2 | Tandem mass spectrometric identification of purified neurotrophic protein

The LC-MS/MS analysis of the trypsin-digested peptides of the NnCM3RP2 fraction demonstrated 77.76% sequence coverage with alpha-elapitoxin-Nk2a (accession no. P01391) of mass of 7.8 kDa

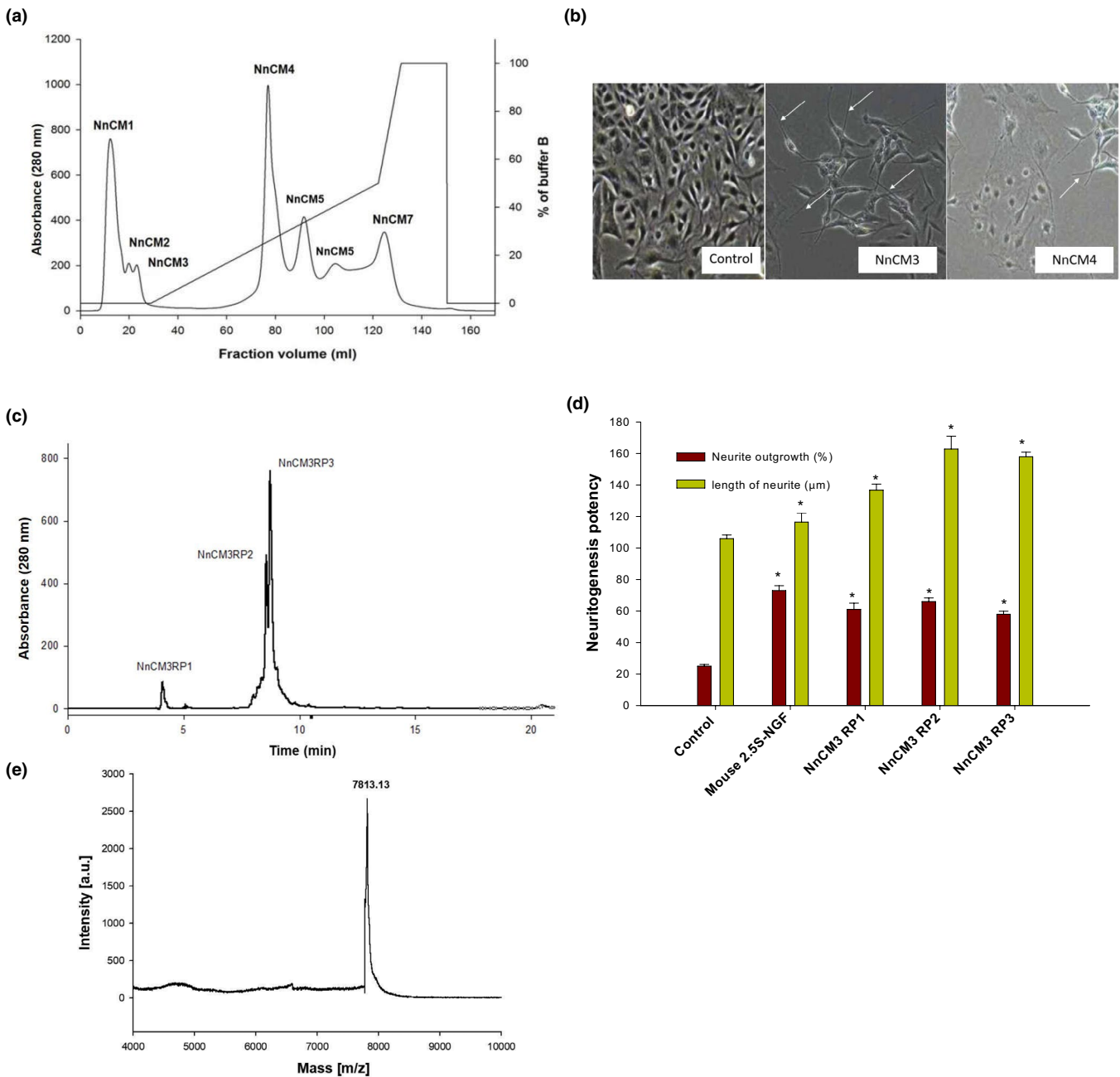


FIGURE 1 (a) Fractionation of crude *N. naja* venom on HiPrep CM FF 16/10 cation exchange column equilibrated with 20 mM Tris-Cl buffer (pH 7.4). The flow rate was set at 1 ml/min and fraction volume of 1.5 ml each was collected. The bound proteins were eluted by 0%–100% linear gradient of 1 M NaCl as mentioned in the text. (b) Screening for neurite outgrowth in pheochromocytoma cell line (PC-12) cells treated with NnCM3 and NnCM4 fractions (100 ng/ml) post 14 days of incubation at 37°C, 5% CO₂. The cells were observed under a phase contrast microscope at 40x magnification. The appearance of neurite outgrowth from PC-12 cells is indicated by arrows. (c) The reversed-phase ultrahigh performance chromatography (RP-UHPLC) purification of NnCM3 fraction on a C₁₈ (Acclaim 300, 4.6 × 150 mm, 3 μm) column. The flow rate of eluting solvent (0.1% v/v trifluoroacetic acid in 90% v/v acetonitrile) was 0.5 ml/min and 250 μl fraction was collected. Bound proteins were eluted using a multistep gradient from 5% to 100% eluting solvent as mentioned in the text. (d) Induction of neurite outgrowth in PC12 cells treated with RP-UHPLC purified fractions [NnCM3RP1 to NnCM3RP3] from *N. naja* venom. Average neurite outgrowth per cell (in μm) and percent of cells showing neurite outgrowth were determined using MOTIC IMAGE PLUS 3.0 software. Significance of difference with respect to control cells, * $p < .05$. (e) Determination of purity and molecular mass of NnCM3RP2 (5 μg) by MALDI-TOF-MS analysis. A 4,800 MALDI TOF/TOF™ analyser was used to determine mass of the protein on a linear analysis mode using an acceleration voltage of 25 kV

from monocled cobra *N. kaouthia* venom (Table 1). The multiple sequence alignment of NnCM3RP2 with *Naja spp.* venom proteins deposited in the NCBI database demonstrated significant sequence similarity with long-chain neurotoxin 4 and α -elapitoxin/ α -cobratoxin

from *N. kaouthia* venom, suggesting that the purified protein structurally resembled the long-chain neurotoxin or α -elapitoxin from cobra venom (Table 1). The protein of the NnCM3RP2 fraction was named Nn- α -elapitoxin-1. Interestingly, it did not demonstrate

TABLE 1 Multiple sequence alignment of Nn- α -elapitoxin-1 with other homologous proteins of *Naja* sp. venom retrieved from National Center for Biotechnology Information (NCBI) databases.

*Indicates identical residues in all sequences; (:) = highly conserved; (.) = moderately conserved.

Name	Accession No.	Sequence Alignment	
Nn- α -elapitoxin-1	Present study	IRCFITPDITS-----KTWCDAFCSIR--RVDLGCAATCPTVKTGVDIQCCSTD	47
Long neurotoxin 4	P25672.1	IRCFITPDITSKDCPNGHVICYKTWCDGFCRIRGERVDLGCAATCPTVKTGVDIQCCSTD	60
Long neurotoxin 5	P25673.1	IRCFITPDITSKDCPNGHVICYKTWCDGFCSSRGERVDLGCAATCPTVKTGVDIQCCSTD	60
toxin B	Prf 764177A	IRCFITPDITSKDCPNGHVICYKTWCDGFCSSRGERVDLGCAATCPTVKTGVDIQCCSTD	60
Long neurotoxin 1	P25668.1	IRCFITPDITSKDCPNGHVICYKTWCDGFCSSRGERVDLGCAATCPTVKTGVDIQCCSTD	60
Long neurotoxin 2	P25669.0	IRCFITPDITSKDCPNGHVICYKTWCDGFCSSRGERVDLGCAATCPTVKTGVDIQCCSTD	60
Alpha-cobratoxin	P01391.1	IRCFITPDITSKDCPNGHVICYKTWCDAFCSIRGKRVLDLGCAATCPTVKTGVDIQCCSTD	60
Long neurotoxin 3	P25671.1	IRCFITPDITSKDCPNGHVICYKTWCDAFCSIRGKRVLDLGCAATCPTVKTGVDIQCCSTD	60

		***** ** *	

Nn- α -elapitoxin-1	Present study	NCNPFPTR---	55
Long neurotoxin 4	P25672.1	DCDPFPTRKR	71
Long neurotoxin 5	P25673.1	DCDPFPTRKR	71
toxin B	Prf 764177A	DC-PFPTRKR	70
Long neurotoxin 1	P25668.1	DCDPFPTRKR	71
Long neurotoxin 2	P25669.0	DCDPFPTRKR	71
Alpha-cobratoxin	P01391.1	NCNPFPTRKR	71
Long neurotoxin 3	P25671.1	DCDPFPTRKR	71
		* * *****	

sequence similarity with conventional NGFs from snake venom or mouse submaxillary gland (Table S1).

3.3 | Nn- α -elapitoxin-1 predominantly binds and induces the internalization of PC-12 cell surface TrkA receptor

Pre-incubation of PC-12 cells with anti-TrkA antibodies resulted in a marked inhibition of binding of Nn- α -elapitoxin-1 and mouse

2.5S-NGF to the PC-12 cells. Nevertheless, blocking of TrkB, TrkC, and p⁷⁵NTR receptors with their respective antibodies did not influence the binding of Nn- α -elapitoxin-1 to the PC-12 cells (Figure 2a). From the regression equation of the dose-response curve, the IC₅₀ value of anti-TrkA antibodies that causes 50% inhibition of binding of Nn- α -elapitoxin-1 and 2.5S-NGF to PC-12 cells was determined to be 5.634 nM and 4.889 nM, respectively.

The binding of FITC conjugated Nn- α -elapitoxin-1 and mouse 2.5S-NGF to PC-12 (Figure 2b), MCF-7 and MDA-MB-231 (Figure S7a,b) cells expressing TrkA receptor post 240 min of incubation was

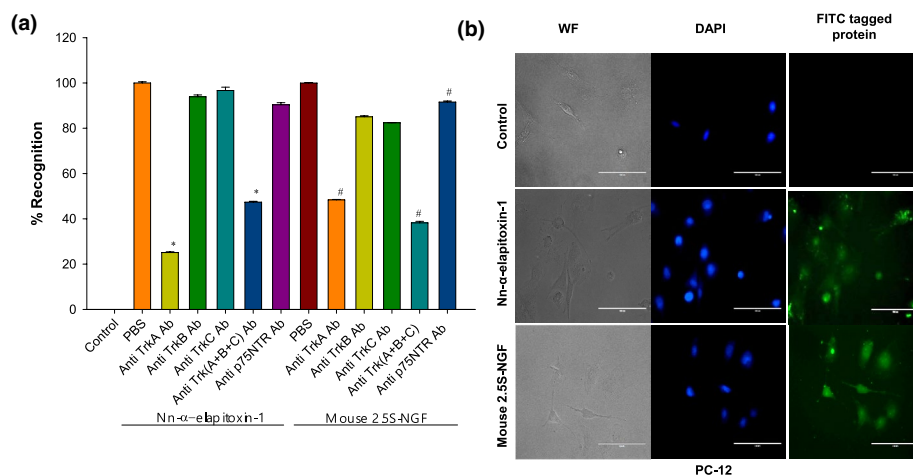


FIGURE 2 (a) Determination of binding of Nn- α -elapitoxin-1 and mouse 2.5S-nerve growth factor (NGF) to TrkA, TrkB, TrkC, and p⁷⁵NT receptors in pheochromocytoma cell line (PC-12) cells either in presence or absence of receptor-specific polyclonal antibodies. The binding of a specific ligand (Nn- α -elapitoxin-1 or mouse 2.5S-NGF) with the control (PBS, phosphate-buffered saline-treated) PC-12 cell was considered as 100% binding, and the binding of the same ligand in the presence of receptor-specific antibodies was compared with that value. Significance of difference with respect to binding ligands in presence of anti-TrkA antibody, for Nn- α -elapitoxin-1, * p < .05; for mouse 2.5S-NGF, # p < .05. (b) Fluorescence microscopic observation of binding of fluorescein isothiocyanate (FITC) tagged Nn- α -elapitoxin-1 and mouse 2.5S-NGF (1 μ g/ml) post 240 min of incubation with PC-12 cells. Magnification was 40X, WF, white field; DAPI, 4',6-diamidino-2-phenylindole

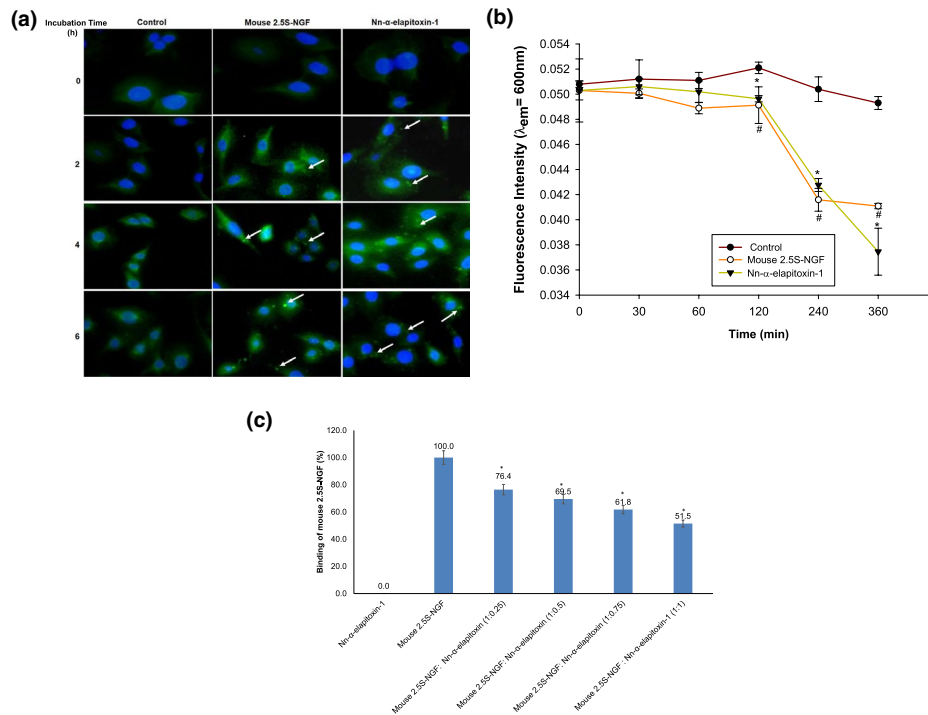


FIGURE 3 Time-dependent (0–360 min) internalization of TrkA receptor of pheochromocytoma cell line (PC-12) cells post binding to 100 ng/ml of Nn- α -elapitoxin-1 and mouse 2.5S- nerve growth factor (NGF) (positive control). (a) Fluorescence microscopic observation of internalization of TrkA receptor to PC-12 cell cytoplasm. Magnification 40x. The arrow indicates internalization of TrkA receptor to the cell cytoplasm. (b) Fluorescence plate reader assay to determine the decrease in cell surface TrkA receptor post treatment with ligands. Significance of difference with respect to control in PC-12 cells at a given time-point; for Nn- α -elapitoxin-1, * $p < .05$, for mouse 2.5S-NGF, # $p < .05$. (c). Competitive ELISA to determine the binding of Nn- α -elapitoxin-1 and mouse 2.5S-NGF to cytosolic domain of recombinant human TrkA receptor. The TrkA receptor (3 nM) was coated to ELISA plate and different ratios of Nn- α -elapitoxin-1 and mouse 2.5S-NGF were added. The binding of mouse 2.5S-NGF was determined by anti-NGF antibody which did not show immunological cross-reactivity with Nn- α -elapitoxin-1. Values are mean \pm SD of triplicate determinations. Significance of difference with respect to binding of only mouse 2.5S-NGF, * $p < .05$

observed under the fluorescence microscope; however, the fluorescence intensity of MCF-7 cells compared to MDA-MB-231 cells was higher. Conversely, no fluorescence signal was detected in L6 and HEK-293 cells (Figure 7c,d).

The immunofluorescence microscopic study showed that both mouse 2.5S-NGF (positive control) and Nn- α -elapitoxin-1 induced internalization of the PC-12 cell surface TrkA receptor in a time-dependent manner (Figure 3a). The results of immunofluorescence microplate reader assay also demonstrated that a concomitant decrease in PC-12 cell surface TrkA receptors was initiated after 2 hr of incubation with Nn- α -elapitoxin-1/mouse 2.5S-NGF. A gradual decline in the receptor concentration was observed post 2 hr of treatment with Nn- α -elapitoxin-1/mouse 2.5S-NGF (Figure 3b).

3.4 | Characterization for the binding of Nn- α -elapitoxin-1 to the recombinant TrkA receptor

Both mouse 2.5S-NGF (positive control) and Nn- α -elapitoxin-1 induced a concentration-dependent decrease in fluorescence

intensity of cytosolic domain of recombinant TrkA receptors at ~ 310 nm, suggesting a strong protein-protein interaction (Figure S8a,b).

The competitive ELISA between Nn- α -elapitoxin-1 and mouse 2.5S-NGF for binding to cytosolic domain of TrkA receptor is shown in Figure 3c. At a 1:1 ratio (Nn- α -elapitoxin-1:2.5S-NGF), the binding of 2.5S-NGF to TrkA receptors was decreased to 50% of its original binding value (100%) (Figure 3c).

3.5 | The anti-TrkA antibody and chemical inhibitor of TrkA receptor inhibit the Nn- α -elapitoxin-1 induced neuritogenesis in PC-12 cells

Pre-incubation of PC-12 cells with anti-TrkA antibodies or with K252a (chemical inhibitor of TrkA) resulted in the abrogation of neuritogenesis potency of Nn- α -elapitoxin-1 and mouse 2.5S-NGF (positive control) (Figure 4a). Nevertheless, addition of anti-TrkA/TrkB/TrkC/p⁷⁵NTR antibodies or K252a in PC-12 cell culture after 1 hr treatment with Nn- α -elapitoxin-1 or mouse 2.5S-NGF did not influence their neuritogenesis potency (Figure 4b).

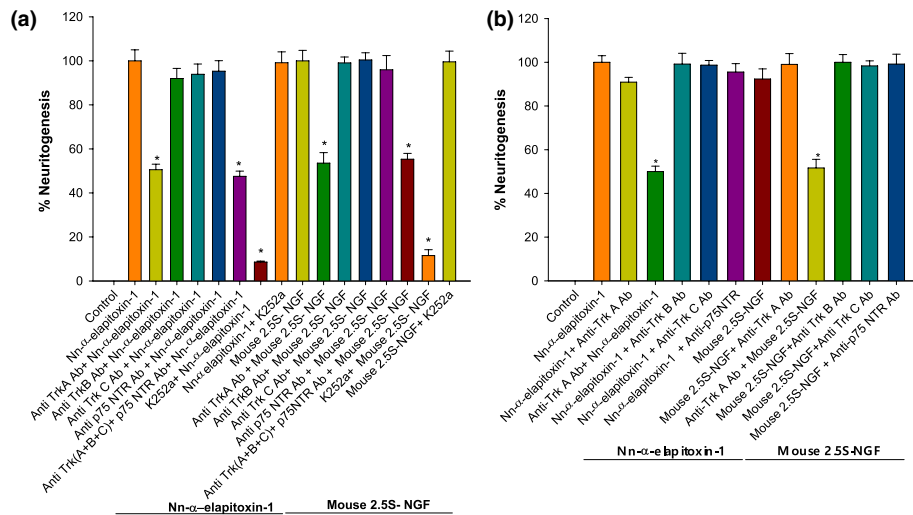


FIGURE 4 Effect of anti-TrkA antibody and chemical inhibitor of TrkA receptor on neuritogenesis of pheochromocytoma cell line (PC-12) cells by neurotrophins. (a) The PC-12 cells were incubated with receptor-specific antibodies against TrkA/B/C and p⁷⁵NTR receptors/chemical inhibitor of TrkA receptor (K252a)/1X phosphate-buffered saline (PBS) (control) followed by treatment with Nn- α -elapitoxin-1 and mouse 2.5S-nerve growth factor (NGF) (positive control). (b) The PC-12 cells were incubated with Nn- α -elapitoxin-1/mouse 2.5S-NGF for 1 hr followed by incubation with receptor-specific antibodies. The neuritogenesis induced by Nn- α -elapitoxin-1/mouse 2.5S-NGF in 1x PBS treated cells was considered as 100% activity and other values were compared to that. Significance of difference with respect to Nn- α -elapitoxin-1 treated PC-12 cells in the absence of any antibody, * $p < .05$; significance of difference with respect to mouse 2.5S-NGF-treated PC-12 cells in the absence of any antibody, # $p < .05$

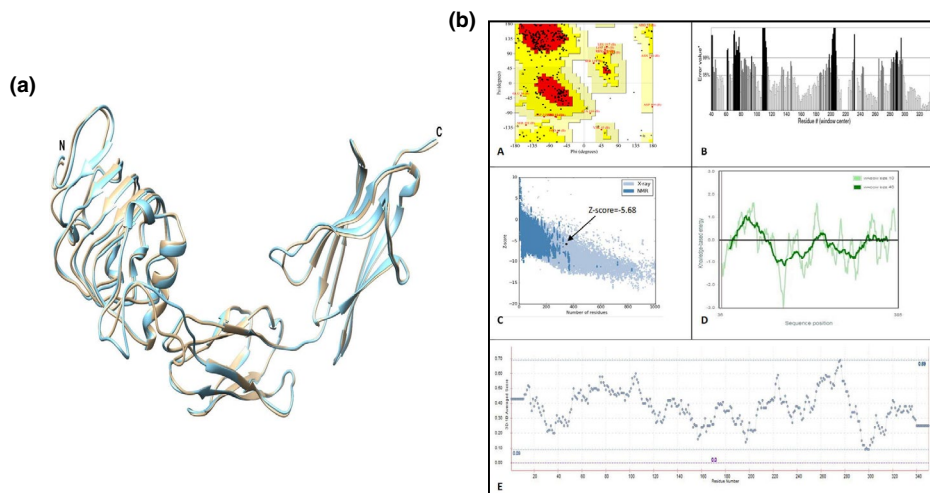


FIGURE 5 Computational (in silico) modelling of TrkA receptor. (a) Superposition structure of model TrkA receptor (cyan) and template (tan). (b) Selected parameters used for model validations of TrkA receptor from *Rattus norvegicus* - (A) Ramachandran Plot, (B) ERRAT score plot, (C) Z-score plot, (D) PROSA knowledge based energy, and (E) Verify 3D score plot

3.6 | Computational (in silico) molecular dynamics simulations of TrkA receptor with cobra venom long-chain α -neurotoxin (1CTX) and mouse NGF (1BET)

The extracellular domain of TrkA receptor was modeled using the human TrkA structure as a template that showed a sequence similarity of 78.9% with rat TrkA sequence (uniprot ID: P35739). The total energy of the protein after energy minimization was determined at -15068.625 kJ/mol. The model structure of TrkA was super positioned with the human TrkA template which showed a RMSD of 0.936 Å (Figure 5a). The quality of the model was ascertained by

choosing various parameters- Ramachandran plot, ERRAT score, Profiles-3D, Knowledge-based energy and Z-score (Figure 5b, Table S2a). The Ramachandran plot showed 66.8% of residues in most favored region with no residues in disallowed region. The phi-psi plot together with other parameters indicates that the model structure is optimum for further analysis. The ligand-receptor complex models formed by interaction of modeled TrkA receptor and ligands 1BET are shown in Figure S9a,b, while the interface residues taking part in the interaction between ligand-receptor complex of extracellular domain of TrkA receptor and 1CTX are shown in Figure S9c,d. The PATCHDOCK results revealed that the modeled TrkA receptor

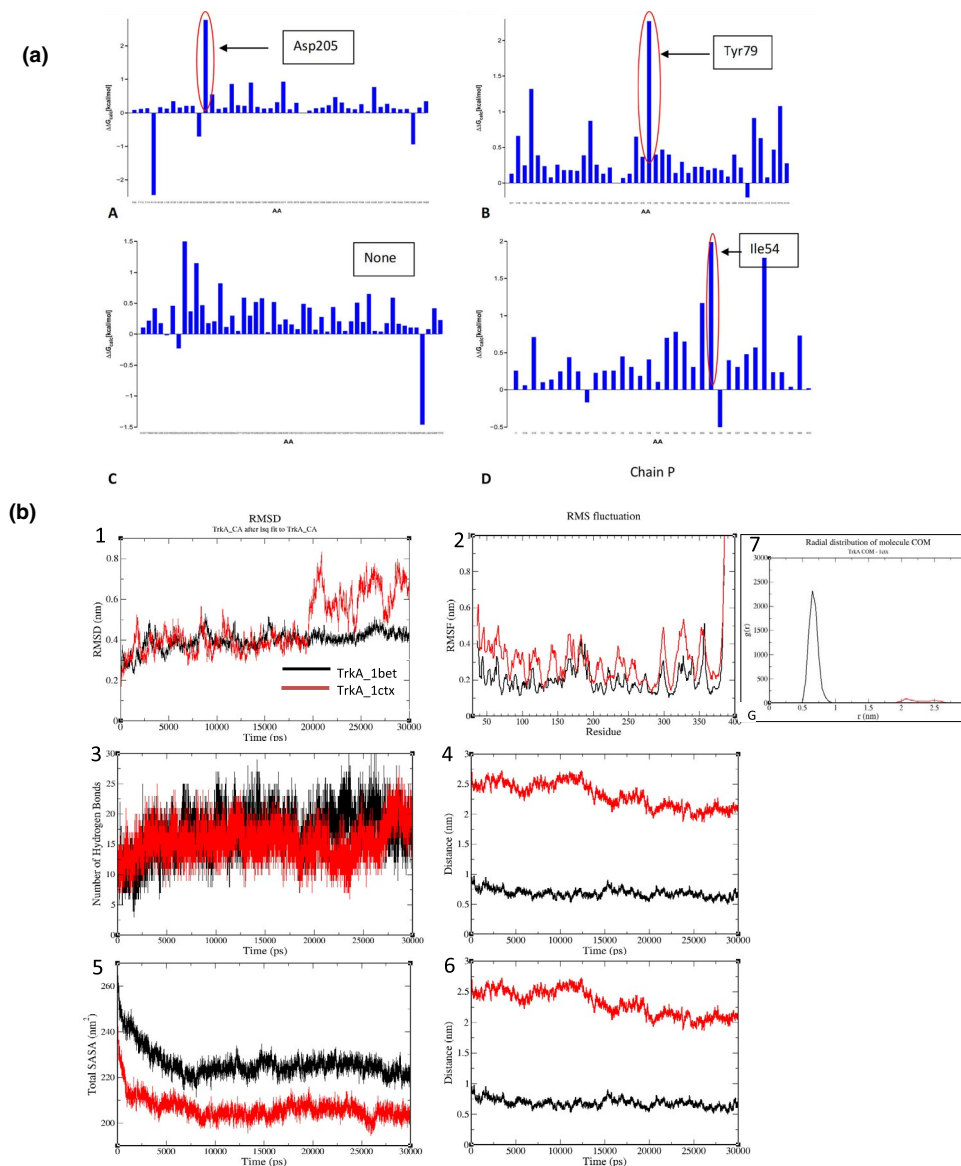


FIGURE 6 (a) Computational (in-silico) alanine scanning mutagenesis to study TrkA-ligand (neurotrophin) interactions to form a complex. (A) TrkA receptor (TrkA_NGF complex), (B) NGF (TrkA_NGF complex), (C) Trk A receptor (TrkA_neurotoxin toxin complex), and (D) Cobra venom neurotoxin (TrkA_neurotoxin toxin complex). (b) MD simulation results showing (1) Root mean square deviation plot versus. time (ps), (2) Root mean square fluctuation plot versus. residue number, (3) number of intermolecular hydrogen bonds versus. time (ps), (4) Radius of gyration plot versus. time (ps), (5) total solvent accessible surface area (nm²) versus. time (ps), (6) distance (nm) versus. time (ps), and (7) radial distribution function plot versus. time (ps). NGF, nerve growth factor

interacts with 1BET with a geometric shape complementarity score of 15,194, approximate interface area of 1925.50, and atomic contact energy (ACE) of 300.66 (Table S2b). Nonetheless, the modeled TrkA receptor interacts with 1CTX with a geometric shape complementarity score of 14,390, approximate interface area of 1949.30, and ACE of -370.34.

The molecular dynamics study revealed the possible hot-spot residues (Figure 6a) across the interface of complexes between extracellular segment of modeled TrkA receptor and ligands 1BET and 1CTX. The total number of interface residues in TrkA-1BET complex was 32 and 30 in TrkA and 1BET, respectively (Figure S9a,b). Furthermore, the interface area for each monomer was found to be 1647 Å² and 1541 Å² for the modeled TrkA and 1BET, respectively

(Table S3). The total number of interface residues in modeled TrkA-1CTX was found to be 34 and 25 in TrkA and 1CTX, respectively (Figure S9c,d). Furthermore, the interface area for each monomer was found to be 1,350 and 1557 Å², respectively (Table S3).

To gain further insights into the energetic contribution of each of the interface residues involved in protein-protein complex formation, in silico alanine scanning mutagenesis was performed for each protein-protein complex between modeled TrkA receptor with 1BET and 1CTX (Figure 6a). The potential hot-spots identified in protein complex formed between TrkA receptor and 1BET was Asp205 of TrkA receptor and Tyr79 of 1BET. The potential hot spots identified in protein complex formed between TrkA receptor and 1CTX were none from TrkA receptor and Ile54 of CTX.

The average geometrical properties of the protein-peptide complexes TrkA-1BET and TrkA-1CTX during 20 ns MD simulation are summarized in Table S4. The modeled TrkA receptor shows more fluctuations, especially after 20 ns when it interacts with 1CTX, whereas the same receptor shows fluctuation within the stable limit throughout the simulation time period when it interacts with 1BET (Figure 6b.1). The RMSD plot shows that TrkA-1BET is more stable compared to TrkA-1CTX and the former undergoes less conformational changes than TrkA-1CTX. The residue wise contribution to the fluctuation analysis by root mean square fluctuation plot shows that the TrkA-1CTX demonstrates higher amplitudes of fluctuation than TrkA-1BET (Figure 6b.2). The TrkA-1BET has higher number of intermolecular H-bonds than TrkA-1CTX which indicates that the interaction between TrkA and 1BET is stronger than that between TrkA and 1CTX (Figure 6b.3). The compactness of both the systems as evaluated using R_g plot showed that the TrkA-CTX is more compact than TrkA-1BET. This indicates that because of high compactness of the latter the interaction of TrkA with α -elapitoxin is weaker than the interaction of TrkA with 2.5S-NGF (Figure 6b.4). The TrkA-1BET has larger area accessible to solvent than TrkA-1CTX (Figure 6b.5) which corroborates with R_g data. The average distance between center of mass of TrkA and 1BET is <1 nm whereas between TrkA and 1CTX is <2.5 nm which again indicates that interaction between TrkA and 1BET is stronger than that between TrkA and 1CTX (Figure 6b.6). The RDF plot shows a sharp peak within a range of 0.5 to 0.9 nm in case of TrkA-1BET whereas in case of TrkA-1CTX a small peak is seen within a range of 1.9 to 2.6 nm (Figure 6b.7) which indicates that TrkA interacts with 1BET more strongly than it does with 1CTX.

3.7 | Comparative transcriptomic analysis of PC-12 cells treated with Nn- α -elapitoxin-1 and mouse 2.5S NGF

The three cDNA libraries obtained from PC-12 cells treated with Nn- α -elapitoxin-1, mouse 2.5S-NGF (positive control), and 1X PBS (control) were sequenced with the Illumina Novoseq 6,000 platform. The

averaged triplicate runs denoting the 20,007,314, 16,640,641, and 16,828,904 raw reads were obtained from Nn- α -elapitoxin-1-treated, control, and mouse 2.5S-NGF-treated PC-12 cells, respectively (Table 2). These cleaned-up reads were obtained after pre-processing (adaptor removal, quality trimming, and N removal) of the raw reads and eliminating the low-quality and empty reads. The re-alignment of the cleaned reads to the latest version of the *Rattus norvegicus* (accession No. GCF_000001895.5) whole genome data showed a very high degree of alignment, ranging from 93% to 94% (Table 2).

The differential expression of PC-12 cell genes post-treatment with mouse 2.5S-NGF and Nn- α -elapitoxin-1 is shown in Tables S5 and S6, respectively. By the transcriptomic analysis, a total of 549 genes were found to be differentially expressed in PC-12 cells post-treatment with mouse 2.5S NGF, compared to the control PC-12 cells. Among these, only 18 genes were found to be significantly up-regulated (fold change >2 and q value <0.6) (Table S5a). Another 185 up-regulation genes were found with a fold change >2, but q values were greater than 0.6 (a q value <0.6 was considered significant) (Table S5b). In contrast, 35 genes in the PC-12 cells were found to be significantly down-regulated (fold change <-2 and q value <0.6) post-addition of mouse 2.5S NGF (Table S5c). The down-regulation of 311 other genes, compared to control cells, was statistically significant (fold change <-2 and q value >0.6) (Table S5d).

The PC-12 cells treated with Nn- α -elapitoxin-1 demonstrated a differential expression of 445 genes; 38 genes exhibited significant up-regulation (fold change >2 and q value <0.6) (Table S6a), whereas 138 genes had a higher expression than normal (fold change >2 and q value >0.6) (Table S6b). In sharp contrast, 32 genes of the PC-12 cells were significantly down-regulated post-treatment with Nn- α -elapitoxin-1 (fold change <-2 and q value <0.6) (Table S6c), whereas 237 genes demonstrated down-regulation but could not be statistically verified (fold change <-2 and q value >0.6) (Table S6d).

A total of 61,578 transcripts vouched for the differential expression of genes between mouse 2.5S-NGF and Nn- α -elapitoxin-1 treated PC-12 cells (data not shown). A heat map of 160 transcripts demonstrating 5-fold or higher differential gene expression in PC-12 cells post-treatment with mouse 2.5S-NGF and Nn- α -elapitoxin-1 is shown in Figure S10a. The heat maps showing differential gene

Sample	Nn- α -elapitoxin-1 treated	Control	Mouse 2.5S-NGF treated
Clean sequencing reads			
Paired reads	18,683,653.67	15,422,006	15,438,910.33
Unpaired reads	1,323,660.667	1,218,635	1,389,993.667
Total reads	20,007,314.33	16,640,641	16,828,904
Total bases (bp)	5,441,604,113	4,528,989,314	4,534,254,276
Alignment statistics			
Total reads	20,007,314.33	16,640,641	16,828,904
Reads aligned	18,827,912	15,595,234.67	15,726,657.67
% reads aligned	94.1	93.74	93.46

TABLE 2 Summary of assembly statistics for the transcriptomic data. The data represent the average of three replicates done under identical experimental conditions

Abbreviation: NGF, nerve growth factor.



expression in PC-12 cells treated with Nn- α -elapitoxin-1/mouse 2.5S-NGF, compared to control PC-12 cells, are shown in Figure S10b,c and Tables S5a,d and S6a,d.

3.8 | A comparative proteomic analysis to identify differentially expressed intracellular proteins in PC-12 cells post treatment with mouse 2.5S-NGF and Nn- α -elapitoxin-1

The LC-MS/MS analysis demonstrated the global expression of intracellular proteins, several of which are common to both neurotrophins-treated and untreated (control) cells (Tables S7a). In addition, the expression of unique intracellular proteins in PC-12 cells post-treatment with mouse 2.5S-NGF and Nn- α -elapitoxin-1, compared to control cells (untreated), were also identified (Tables S7b,d). The diverse biological functions of the identified proteins are also summarized in Tables S7a,d.

From the proteomic analysis, 1,181 intracellular proteins were identified in control (1X PBS treated PC-12 cells), 949 intracellular proteins were identified in Nn- α -elapitoxin-1-treated PC-12 cells, and 777 intracellular proteins were identified in mouse 2.5S-NGF-treated (positive control) PC-12 cells (Figure S11). In particular, 640 intracellular proteins were found in common among all of the cells (Table S7a). The changes in each of these protein entries were manifest as 0.5 to 1.9-fold changes for Nn- α -elapitoxin-1-treated and mouse 2.5S-NGF-treated PC-12 cells, compared to controls (Table S7a).

Interestingly, 106, 40 and 313 intracellular proteins were uniquely expressed in PC-12 cells treated with Nn- α -elapitoxin-1, mouse 2.5S-NGF and 1x PBS (control), respectively (Tables S7b,d).

3.9 | The transcriptomics and functional proteomics analyses in unison show common and unique pathways of neuritogenesis between Nn- α -elapitoxin-1 and mouse 2.5S-NGF

The functional proteomics data and the transcriptomics analysis explicitly show the common and differential expression of transcripts and intracellular proteins associated with cellular differentiation and the neuritogenesis pathways by Nn- α -elapitoxin-1 and mouse 2.5S-NGF. Taken together, the data from the analyses show the up-regulation of 35 signaling pathways in PC-12 cells (Table 3), while 23 signaling pathways were down-regulated (Table 4), post-treatment with mouse 2.5S-NGF and Nn- α -elapitoxin-1. The combined data from the transcriptomics, proteomics, and inhibitors on the different cellular signaling pathways (see below) suggest that microtubule associated protein kinase (MAPK) is the major pathway for neuritogenesis by both Nn- α -elapitoxin-1 and mouse 2.5S-NGF.

The transcriptomics and proteomic studies demonstrated that mouse 2.5S-NGF uniquely up-regulates the genes corresponding to purine metabolism (Höpker, Saffrey, & Burnstock, 1996) and the JAK/STAT pathway (Edman, Mira, & Arenas, 2008) leading to the

higher synthesis of protein (Uniprot ID- Q8R414, P09330) in PC-12 cells. This suggests the involvement of mouse 2.5S-NGF in these pathways in the neuritogenesis process. Some key components of integrin signaling and inflammation are also found to be uniquely down-regulated by mouse 2.5S-NGF, resulting in lower protein synthesis (Uniprot ID- D3Z8L7, D3Z8L7, A0A0G2K7A5) (Table 5).

While certain key genes in the heterotrimeric G-protein signaling pathway (RGD=619751), cytokine-mediated inflammation pathway (RGD=619751), and fibroblast growth factor (FGF) signaling pathway (RGD=620164) are involved in neuritogenesis, they are uniquely up-regulated in Nn- α -elapitoxin-1-treated PC-12 cells, compared to control cells. The proteins (Uniprot ID- O88302, Q9ERW3) associated with these genes are directly or indirectly linked to the expression of the MAP kinase pathway (Table 6). Nevertheless, the genes related to apoptosis (RGD=1593284) and disease-related pathways in PC-12 cells are down-regulated by Nn- α -elapitoxin-1 (Table 6).

3.10 | Validation of Nn- α -elapitoxin-1-induced major signaling pathway(s) in PC-12 cells by western blot analysis

The 2.3 and 1.3 fold increase in the relative expression for the phosphorylation of p38 and extracellular signal-regulated kinase (ERK1/2), respectively in Nn- α -elapitoxin-1-treated PC-12 cells confirms the activation of the MAPK pathway during neuritogenesis (Figure 7a,b). This was further supported by the fact that addition of MAPK inhibitors (U0126 and PD98059) to PC-12 cells prior to the addition of Nn- α -elapitoxin-1 or mouse 2.5S-NGF (positive control) resulted in a significant reduction in the neuritogenesis ability of these neurotrophins (Table 7). Nevertheless, the above chemical inhibitors of the MAPK pathway differentially inhibited ($p < .05$) the neuritogenesis potency of the neurotrophin molecules under study (Table 7).

The 1.14-fold increase in CREB and the ~2-fold elevation in the relative expression of P-CREB signaling proteins in Nn- α -elapitoxin-1-treated PC-12 cells points to the activation of the PKC signaling pathway (Figure 7a,b). The chemical inhibitor of the PKC signaling pathway (Go6976) inhibited the Nn- α -elapitoxin-1 or mouse 2.5S-NGF mediated neuritogenesis of PC-12 cells, though to significantly ($p < .05$) different extents (Table 7), indicating their differential activation of the PKC signaling pathway.

The Nn- α -elapitoxin-1 induced 1.7 fold increase in the relative expression of phosphorylated Akt protein in treated PC-12 cells, compared to control cells (Figure 7a,b), suggesting the involvement of phosphoinositide 3-kinase (PI3K)/Akt signaling pathway(s) in the Nn- α -elapitoxin-1-mediated neuritogenesis process in PC-12 cells. In addition, LY294002, an inhibitor of the PI3K/Akt pathway, was also able to reduce the neuritogenesis induced by mouse 2.5S-NGF (positive control) and by Nn- α -elapitoxin-1, by 35% and 45%, respectively, compared to their original neuritogenesis activity in PC-12 cell (Table 7). On the other hand, the JNK inhibitor did not influence the

TABLE 3 Common up-regulated pathways in PC-12 cells, as determined by both proteomics and transcriptomics analyses, post treatment with mouse 2.5S-NGF (positive control) and Nn- α -elapitoxin-1

Pathway accession number	Mapped IDs of pathways	Involvement of protein the pathway
P04374	RAT RGD=69319 UniProtKB=P54313	5HT2 type receptor mediated signaling pathway
P00003	RAT RGD=62087 UniProtKB=P27704	Alzheimer disease-amyloid secretase pathway
P00004	RAT RGD=1597195 UniProtKB=D4A9J2, RAT RGD=621320 UniProtKB=P50282	Alzheimer disease-presenilin pathway
P00005	RAT RGD=62087 UniProtKB=P27704, RAT RGD=1597195 UniProtKB=D4A9J2	Angiogenesis
P05911	RAT RGD=69319 UniProtKB=P54313	Angiotensin II-stimulated signaling through G proteins and beta-arrestin
P00006	RAT RGD=621280 UniProtKB=Q92412, RAT RGD=620963 UniProtKB=P68101, RAT RGD=621282 UniProtKB=F7FLN8	Apoptosis signaling pathway
P00012	RAT RGD=1597195 UniProtKB=D4A9J2	Cadherin signaling pathway
P06959	RAT RGD=621320 UniProtKB=P50282, RAT RGD=621282 UniProtKB=F7FLN8	CCKR signaling map
P05912	RAT RGD=69319 UniProtKB=P54313	Dopamine receptor mediated signaling pathway
P00018	RAT RGD=1585097 UniProtKB=A0A0G2JZD1	EGF receptor signaling pathway
P00019	RAT RGD=68436 UniProtKB=P19686, RAT RGD=71014 UniProtKB=Q04400	Endothelin signaling pathway
P00021	RAT RGD=620164 UniProtKB=Q9ERW3	FGF signaling pathway
P06664	RAT RGD=621280 UniProtKB=Q92412, RAT RGD=69319 UniProtKB=P54313	Gonadotropin releasing hormone receptor pathway
P00026	RAT RGD=69319 UniProtKB=P54313, RAT RGD=71014 UniProtKB=Q04400	Heterotrimeric G-protein signaling pathway-Gi alpha and Gs alpha mediated pathway
P00027	RAT RGD=619751 UniProtKB=O88302	Heterotrimeric G-protein signaling pathway-Gq alpha and Go alpha mediated pathway
P00028	RAT RGD=69319 UniProtKB=P54313	Heterotrimeric G-protein signaling pathway-rod outer segment phototransduction
P04385	RAT RGD=69319 UniProtKB=P54313	Histamine H1 receptor mediated signaling pathway
P00029	RAT RGD=2736 UniProtKB=P35439, RAT RGD=2661 UniProtKB=P04797	Huntington disease
P00031	RAT RGD=619751 UniProtKB=O88302	Inflammation mediated by chemokine and cytokine signaling pathway
P00034	RAT RGD=62087 UniProtKB=P27704, RAT RGD=2375 UniProtKB=P05539, RAT Ensembl=ENSRNOG00000048449 UniProtKB=M0RCF3	Integrin signaling pathway
P00036	RAT RGD=62087 UniProtKB=P27704	Interleukin signaling pathway
P00037	RAT RGD=2736 UniProtKB=P35439	Ionotropic glutamate receptor pathway
P00041	RAT RGD=619751 UniProtKB=O88302	Metabotropic glutamate receptor group I pathway
P00040	RAT RGD=69319 UniProtKB=P54313	Metabotropic glutamate receptor group II pathway
P00042	RAT RGD=69319 UniProtKB=P54313, RAT RGD=2736 UniProtKB=P35439	Muscarinic acetylcholine receptor 1 and 3 signaling pathway
P06587	RAT RGD=2350 UniProtKB=P12390	Nicotine pharmacodynamics pathway
P04391	RAT RGD=69319 UniProtKB=P54313	Oxytocin receptor mediated signaling pathway
P00059	RAT RGD=1564788 UniProtKB=F1LTH9	p53 pathway
P00049	RAT RGD=621093 UniProtKB=Q9JHW0	Parkinson disease
P00047	RAT RGD=62087 UniProtKB=P27704	PDGF signaling pathway
P00048	RAT RGD=69319 UniProtKB=P54313	PI3 kinase pathway
P00052	RAT RGD=1591873 UniProtKB=D3ZWC5	TGF-beta signaling pathway
P04394	RAT RGD=69319 UniProtKB=P54313	Thyrotropin-releasing hormone receptor signaling pathway

(Continues)

**TABLE 3** (Continued)

Pathway accession number	Mapped IDs of pathways	Involvement of protein the pathway
P00056	RAT RGD=62087 UniProtKB=P27704	VEGF signaling pathway
P00057	RAT RGD=619751 UniProtKB=O88302	Wnt signaling pathway

Note: These pathways enhance neurogenesis in PC-12 cells (KEGG pathway entry: rno04722).

Abbreviations: KEGG, Kyoto Encyclopedia of Genes and Genomes; NGF, nerve growth factor; PC-12, pheochromocytoma cell line.

TABLE 4 The common down-regulated pathways in PC-12 cells, as determined by both proteomics and transcriptomics analyses, post treatment with mouse 2.5S-NGF (positive control) and Nn- α -elapitoxin-1

Pathway accession	Mapped IDs	Name of the Pathway
P00016	RAT RGD=735144 UniProtKB=O08816	Cytoskeletal regulation by Rho GTPase
P00034	RAT Ensembl=ENSRNOG00000051399 UniProtKB=A0A0G2K7A5	Integrin signaling pathway
P00006	RAT RGD=1593284 UniProtKB=P0DMW0	Apoptosis signaling pathway
P00031	RAT RGD=1311443 UniProtKB=D3Z8L7	Inflammation mediated by chemokine and cytokine signaling pathway
P00029	RAT RGD=735144 UniProtKB=O08816	Huntington disease
P06664	RAT RGD=620436 UniProtKB=P11962	Gonadotropin releasing hormone receptor pathway
P00018	RAT RGD=1311443 UniProtKB=D3Z8L7	EGF receptor signaling pathway
P04394	RAT RGD=620436 UniProtKB=P11962	Thyrotropin-releasing hormone receptor signaling pathway
P00005	RAT RGD=70500 UniProtKB=P63086, RAT RGD=619921 UniProtKB=P61589, RAT RGD=1306884 UniProtKB=Q4KM68	Angiogenesis
P00059	RAT RGD=1306919 UniProtKB=Q5I0H3, RAT RGD=619975 UniProtKB=D3ZVU7	p53 pathway
P00036	RAT RGD=70500 UniProtKB=P63086	Interleukin signaling pathway
P00019	RAT RGD=70500 UniProtKB=P63086, RAT RGD=2716 UniProtKB=Q63803	Endothelin signaling pathway
P04391	RAT RGD=621516 UniProtKB=G3V6P8, RAT RGD=2245 UniProtKB=P22002	Oxytocin receptor mediated signaling pathway
P00027	RAT RGD=619921 UniProtKB=P61589, RAT RGD=621516 UniProtKB=G3V6P8	Heterotrimeric G-protein signaling pathway-Gq alpha and Go alpha mediated pathway
P00057	RAT RGD=621516 UniProtKB=G3V6P8, RAT RGD=1304726 UniProtKB=Q56A18, RAT RGD=1303209 UniProtKB=Q68HB8, RAT RGD=2025 UniProtKB=P68136, RAT RGD=619975 UniProtKB=D3ZVU7	Wnt signaling pathway
P00047	RAT RGD=70500 UniProtKB=P63086, RAT RGD=1306884 UniProtKB=Q4KM68	PDGF signaling pathway
P00042	RAT RGD=621516 UniProtKB=G3V6P8, RAT RGD=2736 UniProtKB=P35439	Muscarinic acetylcholine receptor 1 and 3 signaling pathway
P00012	RAT RGD=1303209 UniProtKB=Q68HB8, RAT RGD=2025 UniProtKB=P68136	Cadherin signaling pathway
P06959	RAT RGD=70500 UniProtKB=P63086, RAT RGD=619921 UniProtKB=P61589	CCKR signaling map
P04385	RAT RGD=621516 UniProtKB=G3V6P8	Histamine H1 receptor mediated signaling pathway
P06587	RAT RGD=2245 UniProtKB=P22002	Nicotine pharmacodynamics pathway
P04374	RAT RGD=621516 UniProtKB=G3V6P8, RAT RGD=2245 UniProtKB=P22002	5HT2 type receptor mediated signaling pathway
P00004	RAT RGD=2025 UniProtKB=P68136	Alzheimer disease-presenilin pathway

Note: The down-regulation of these pathways enhance neurogenesis in PC-12 cells (KEGG pathway entry: rno04722).

Abbreviations: KEGG, Kyoto Encyclopedia of Genes and Genomes; PC-12, pheochromocytoma cell line.

TABLE 5 A comparison of expression of unique proteins between mouse 2.5S-NGF-treated and Nn- α -elapitoxin-1-treated PC-12 cells

Pathway accession	Mapped IDs	Pathway name and/or protein function
Down-regulated		
P00034	RAT Ensembl=ENSRNOG00000051399 UniProtKB=A0A0G2K7A5	Integrin signaling pathway
	RAT RGD=1311443 UniProtKB=D3Z8L7	
P00031	RAT RGD=1311443 UniProtKB=D3Z8L7	Inflammation
Up-regulated		
R-RNO-416476/R-RNO-375276	RAT RGD=620898 UniProtKB=Q8R414	activation of MAPK activity (JAK/STAT signaling pathway)
P02744	RAT RGD=3415 UniProtKB=P09330	purine biosynthetic pathway; pentose phosphate pathway; purine metabolic pathway (Purine metabolism)

Note: The expression of unique proteins was determined by both transcriptomics and proteomics analyses. The up-regulation or down-regulation of proteins in mouse 2.5S-NGF-treated cells is compared to the quantitative expression of the same proteins in control (untreated) cells.

Abbreviations: NGF, nerve growth factor; MAPK, microtubule associated protein kinase; PC-12, pheochromocytoma cell line.

TABLE 6 A comparison of expression of unique proteins between Nn- α -elapitoxin-1-treated and mouse 2.5S-NGF-treated PC-12 cells

Pathway accession No.	Mapped IDs	Pathway name and/or protein function
Down-regulated		
P00016	RAT RGD=735144 UniProtKB=O08816	Cytoskeletal regulation by Rho GTPase
P00006	RAT RGD=1593284 UniProtKB=P0DMW0	Apoptosis signaling pathway
P02740	RAT RGD=70497 UniProtKB=Q05982	De novo pyrimidine ribonucleotides biosynthesis
P00029	RAT RGD=735144 UniProtKB=O08816	Huntington disease
P06664	RAT RGD=620436 UniProtKB=P11962	Gonadotropin releasing hormone receptor pathway
	RAT RGD=1593284 UniProtKB=P0DMW0	
P00049	RAT RGD=1593284 UniProtKB=P0DMW0	Parkinson disease
Up-regulated		
P00027	RAT RGD=619751 UniProtKB=O88302	Heterotrimeric G-protein signaling pathway-Gq alpha and Go alpha mediated pathway
P00031	RAT RGD=619751 UniProtKB=O88302	Inflammation mediated by chemokine and cytokine signaling pathway
P00021	RAT RGD=620164 UniProtKB=Q9ERW3	FGF signaling pathway

Note: The expression of unique proteins was determined by both transcriptomics and proteomics analyses. The up-regulation or down-regulation of proteins in Nn- α -elapitoxin-1 treated cells is compared to the quantitative expression of the same proteins in control (untreated) cells.

Abbreviations: FGF, fibroblast growth factor; NGF, nerve growth factor; PC-12, pheochromocytoma cell line.

neuritogenesis potency of both N- α -elapitoxin-1 and mouse 2.5S-NGF (Table 7).

Western blotting analysis showed a 2.8-fold increase in the basal level relative expression of Bcl-2 in Nn- α -elapitoxin-1-treated PC-12 cells, compared to control cells (Figure 7a,b). Furthermore, treatment of PC-12 cells with Nn- α -elapitoxin-1 did not result in an enhanced expression of P-JNK and BAX proteins, compared to the expression of these proteins in control PC-12 cells (Figure 7a,b). Moreover the JNK inhibitor SP600125 demonstrated a marginal inhibition of neurite outgrowth in PC-12 cells post-treatment with Nn- α -elapitoxin-1 (7.9%) and with mouse 2.5S-NGF (6.5%) (Table 7).

4 | DISCUSSION

Snake venom α -neurotoxins that are routinely used to characterize the nicotinic receptors in vertebrate skeletal muscle and in the electric tissue of electric fish, have been reported to block nicotinic transmission in the neuro-muscular junction (Nirthanan & Gwee, 2004). Although the neuritogenesis ability of snake venom NGF is a well-known phenomenon, this is the first report showing neuritogenesis potency of a Cobra venom alpha-neurotoxin (Nn- α -elapitoxin-1) in PC-12 neuronal cells. The presence of long chain neurotoxin with sequence similarity to Nn- α -elapitoxin-1 has also been demonstrated by whole genome sequencing and/or proteomic

**TABLE 7** Data showing the percent inhibition of neuritogenesis in PC-12 by signaling pathway(s)-specific small synthetic inhibitors

Treatment conditions of PC-12 cells	Inhibitor of signaling pathway	Neuritogenesis (% of PC-12 cells transformed)	P-value
Nn- α -elapitoxin-1	None (control)	100	0.88
Mouse 2.5S-NGF	None (control)	93.8 \pm 2.2	
U0126 (10 μ M) + Mouse 2.5S-NGF	MAPK inhibitor (Erk1 & Erk2)	10.2 \pm 1.4	0.053
U0126 (10 μ M) + Nn- α -elapitoxin-1	MAPK inhibitor (Erk1 & Erk2)	17.6 \pm 0.9	
PD98059 (10 μ M) + Mouse 2.5S-NGF	MAPK inhibitor (Very high to Erk1 & low Erk2)	67.2 \pm 3.4	0.28
PD98059 (10 μ M) + Nn- α -elapitoxin-1	MAPK inhibitor (Very high to Erk1 & low Erk2)	59.1 \pm 3 0.0	
SB203580 (10 μ M) + Mouse 2.5S-NGF	p38 inhibitor	80.5 \pm 4.0	0.03
SB203580 (10 μ M) + Nn- α -elapitoxin-1	p38 inhibitor	96.3 \pm 4.8	
G06976 (3 μ M) + Mouse 2.5S-NGF	PKC inhibitor	74.0 \pm 3.7	0.02
G06976 (3 μ M) + Nn- α -elapitoxin-1	PKC inhibitor	84.9 \pm 4.2	
LY294002(10 μ M) + Mouse 2.5S-NGF	Akt inhibitor	65.0 \pm 3.2	0.28
LY294002(10 μ M) + Nn- α -elapitoxin-1	Akt inhibitor	54.9 \pm 2.7	
H:89 (10 μ M) + Mouse 2.5S-NGF	PKA inhibitor	80.0 \pm 4.0	0.03
H:89 (10 μ M) + Nn- α -elapitoxin-1	PKA inhibitor	52.5 \pm 2.6	
SP600125 (10 μ M) + 2S-Mouse 2.5S-NGF	JNK inhibitor	92.0 \pm 4.6	0.54
SP600125(10 μ M) + Nn- α -elapitoxin-1	JNK inhibitor	93.5 \pm 3.7	

Note: The neuritogenesis induced by Nn- α -elapitoxin-1 in PC-12 cell was considered as 100% activity and other values were compared to that. The control (1X PBS treated) cells showed 17.3% transformation and this value was deducted from the experimental results. Values are mean \pm SD of triplicate determinations. The $p \leq .05$ between two sets of results was considered as statistically significant.

Abbreviations: Erk, extracellular signal-regulated kinase; MAPK, microtubule associated protein kinase; NGF, nerve growth factor; PBS, phosphate-buffered saline; PC-12, pheochromocytoma cell line.

analysis of Indian Cobra *N. naja* venom (Chanda et al., 2018; Chanda & Mukherjee, 2020; Suryamohan et al., 2020).

Neurotrophins modulate the development and maintenance of functional vertebrate nervous systems by activating two different classes of receptors: (a) the Trk family of receptor tyrosine kinases, and (b) p⁷⁵NTR, a member of the tumour necrosis factor receptor superfamily (Huang & Reichardt, 2001; Patapoutian & Reichardt, 2001). Studies have shown the independent functioning of these receptors by low-affinity interactions with neurotrophins/NGF; however, the co-expression of TrkA and p⁷⁵NTR receptors results in high-affinity binding with mammalian NGF to alter the cellular signaling mechanism (Toni, Dua, & van der Graaf, 2014). Furthermore, studies have shown that p⁷⁵NTR plays a major role in regulating neuritogenesis (Bibel, Hoppe, & Barde, 1999; Lad, Williams, & Wolfenden, 2003). A significant difference is seen in the molecular mass and structure of mouse-NGF and Nn- α -elapitoxin-1, so that the latter molecule could bind to the TrkA receptor without requiring p⁷⁵NTR. This suggests a possible difference in the neuritogenesis mechanism for mouse 2.5S-NGF and Nn- α -elapitoxin-1. In any case, similar to mouse 2.5S-NGF, Nn- α -elapitoxin-1 has also been found to be highly specific toward the TrkA receptor subtype of PC-12 cells. This study has provided conclusive evidence that Nn- α -elapitoxin-1 binds to TrkA receptor expressed on the surface of PC-12, MCF-7 and MDA-MB-231 (Descamps et al., 2001); however, the cells such as HEK-293 and L6 lacking this receptor on cell surface do not show binding with Nn- α -elapitoxin-1. Noteworthy, the TrkA acts as the receptor for

mammalian NGF, whereas TrkB preferentially binds with brain-derived neurotrophic factors and NT-4/5, and TrkC is the preferred receptor for neurotrophin-3 (Massa et al., 2010). Furthermore, several prominent structural differences between mammalian NGF and Nn- α -elapitoxin-1, for example, no sequence similarity between conventional NGF from snake venom or mammals and Nn- α -elapitoxin-1, and a significant difference in their size unequivocally suggest that they may also differ in their receptor binding site and/or binding proficiency, and mechanism of binding with TrkA receptor which was subsequently demonstrated by *in silico* analysis.

The computational analysis suggests that mouse 2.5S-NGF (1BET) and Nn- α -elapitoxin-1(1CTX) bind to different epitopes of TrkA receptor and it is quite interesting to note that no common residues are found to be taking part in the interaction of these two neurotrophins originating from diverse biological sources with TrkA receptor. Moreover neurotoxins are very well known for their ability to bind nicotinic acetylcholine receptor (nAChR) to inflict neurotoxicity (Mohan & Yu, 2007). Various studies have reported that long and short-chain postsynaptic neurotoxins adapt a similar folding pattern, consisting of 3 loops- loop 1, loop 2 and loop 3 (Kuo, Chang, & Chang, 1995). The detailed molecular interaction studies on nAChR-binding to neurotoxin have indicated the active participation of several residues, Ser23, Tyr25, Lys27, Trp29, Gln28, Arg43, Gly44, and Lys47, which are of prime functional importance (Kuo et al., 1995). Whereas, in the present study, by alanine scanning mutagenesis and *in silico* interactive study the active residues involved

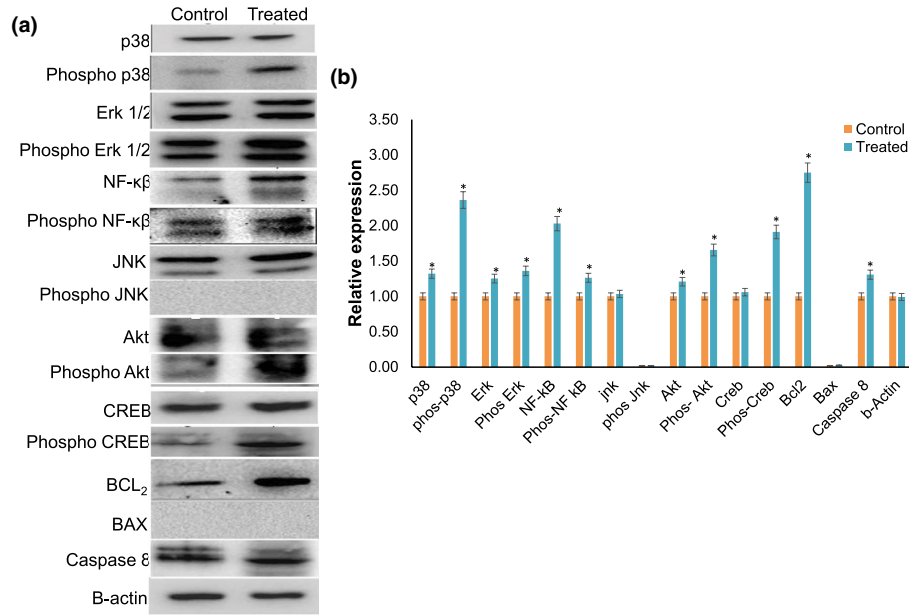


FIGURE 7 (a) Western blot analysis to determine the relative expression of proteins of signaling pathways in Nn- α -elapitoxin-1-treated cells compared to control pheochromocytoma cell line (PC-12) cells. The cells were treated with 100 ng/ml of Nn- α -elapitoxin-1 or 1X phosphate-buffered saline (control) and intracellular proteins were isolated post 14 days of incubation, separated by 12% sodium dodecyl sulfate–polyacrylamide gel electrophoresis and the expressions of desired proteins were detected by immuno blot analysis using antibodies against the targeted proteins. (b) Densitometry analysis of western blots to show the relative expression of intracellular proteins in control and Nn- α -elapitoxin-1-treated PC-12 cells. The expression of proteins was normalized to β -actin using ImageJ software. The values show the mean \pm SD of normalized values for three different experiments. Significance of difference with respect to control, $*p < .05$

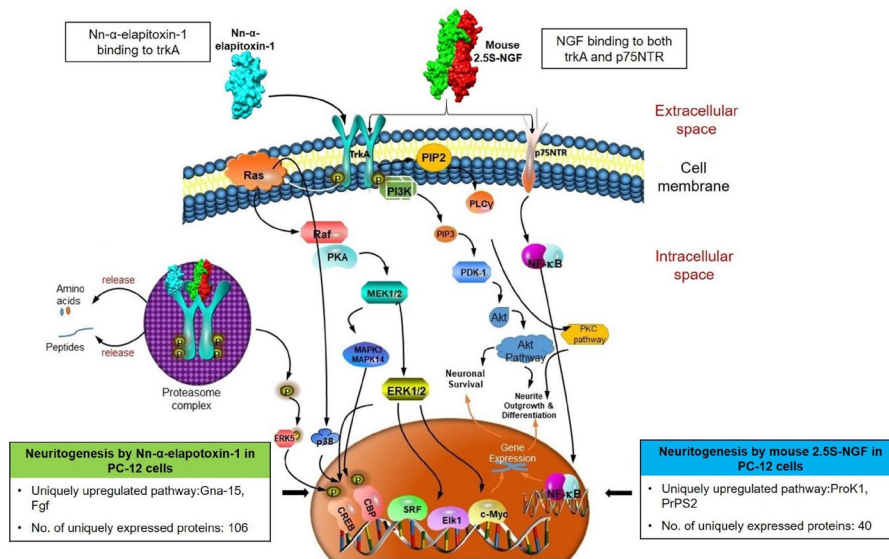


FIGURE 8 Proposed mechanism of neuritogenesis pathways in pheochromocytoma cell line (PC-12) cells by Nn- α -elapitoxin-1 and mouse 2.5S-nerve growth factor (NGF)

in the interaction between neurotoxin (Nn- α -elapitoxin-1) and TrkA are Asp53, Ser31, Lys69, Gly51, and Lys49 residues (shown in Figure S9), and these are found to be different from the residues of the neurotoxin interacting with nAChR (Kuo et al., 1995). Furthermore, the binding site hotspot residues taking part in an interaction between the neurotoxin and TrkA receptor and thus providing a conducive environment for ligand-receptor interaction dictated by in silico

alanine scanning have revealed the key amino acid residues which are of great importance for its functional activity.

This in silico analysis also suggests that the strength of interaction between TrkA and mouse 2.5S-NGF is greater than the interaction between TrkA and Nn- α -elapitoxin-1; however, this differential strength of binding to TrkA receptor or binding to two different epitopes of TrkA receptor by the neurotrophins under study did not



produce any difference in their biological activity, efficacy, and neurogenesis potential in PC-12 cells. Nevertheless, Nn- α -elapitoxin-1-induced signaling leading to neurogenesis in PC-12 cells was slightly distinct than that of mouse 2.5S-NGF-induced signaling as discussed below.

The internalization and transport of a ligand-receptor complex is necessary for commencing cell body responses to target-derived neurotrophins (Song & Yoo, 2011; Zhang, Moheban, Conway, Bhattacharyya, & Segal, 2000). Consequently, the binding of Nn- α -elapitoxin-1 to cell surface TrkA receptor and the subsequent internalization of the receptor-ligand complex into the cell cytoplasm confirm the neuronal differentiation being promoted by catalytically active Trks within the endosomes (Zhang et al., 2000).

PC-12 cells show a rapid response to neurotrophins by differentiating into synaptic-like neuronal cells exerting a thread-like structure from their cell body (known as a neurite), which is quantitatively studied to decipher the interaction between xenobiotic compounds and neurons (Isom & Borowitz, 2016). The neurotrophin-induced neurite outgrowth in PC-12 cells post-binding to the extracellular domain of the TrkA receptor is mediated by three distinct signaling pathways: (i) extracellular signal-regulated kinase 1 (ERK1) and ERK2 (also known as MAPK1), (ii) PI3K-AKT, and (iii) phospholipase C γ (PLC γ) pathways (Chetty, 2019; Harrington & Ginty, 2013). Ligand-mediated activation of TrkA receptors and the subsequent downstream pathways lead to propagation of the signaling stimuli that lead to inhibition of apoptosis, differentiation, and cell survival (Eggert, Sieverts, Ikegaki, & Brodeur, 2000; Zhang et al., 2000).

The present study provides convincing evidences to show that Nn- α -elapitoxin-1 and mouse 2.5S-NGF follow some common pathways of neurogenesis in PC-12 cells, though the expression of neurotrophin (Nn- α -elapitoxin-1 or mouse 2.5S-NGF)-specific unique pathways has also been observed. The two major pathways (MAPK and PI3K) are found in common between Nn- α -elapitoxin-1 and mouse 2.5S-NGF for inducing neurogenesis. Nevertheless, the PLC γ pathway of neurogenesis is uniquely observed in mouse 2.5S-NGF-treated PC-12 cells (Figure 8). The FGF signaling and heterotrimeric G-protein signaling pathways, reported to be involved in neural growth and survival (Loers, Chen, Grumet, & Schachner, 2005), are uniquely expressed in Nn- α -elapitoxin-1-treated PC-12 cells undergoing neurogenesis (Table 6), which suggests that this toxin induces neurogenesis by regulating these two unique pathways. The combined data from transcriptomics and proteomics analyses, inhibition of neurogenesis by pathway-specific chemical inhibitors, and western blot analysis unequivocally demonstrate that MAPK is the major common signal transduction pathway of neurogenesis for both Nn- α -elapitoxin-1 and mouse 2.5S-NGF. This is despite the demonstration that these two diverse neurotrophic molecules can induce nerve growth via some additional and distinct pathways.

The first cascade influenced by activation of TrkA receptor is Ras-mediated activation of the MAPK pathway. MAPKs are intracellular proteins regulated positively via phosphorylation of the cytosolic threonine and tyrosine by MAP kinase

or extracellular signal-regulated kinase (ERK) or kinases MEKS (Cargnello & Roux, 2011). MEK is a part of the serine-threonine protein kinase family that phosphorylates and activates MEKs independently of Raf (Katz, Amit, & Yarden, 2007). Mouse-NGF and several other xenobiotic stimulants are reported to activate the MEK in resting PC-12 cells (Marshall, 1995). In the MAPK pathway, p38 and ERK1/2 are key proteins, and their activation (phosphorylation) carries the signal forward into the nucleus, subsequently regulating the activity of many transcription factors including ETS domain-containing protein ELK1 (Li et al., 2003). The activation of ERK1/2 may also trigger a phosphorylation of ribosomal S6 kinase (S6K) resulting in the generation of the secondary messenger cAMP that subsequently regulates the expression of NGF/neurotrophin-inducible genes responsible for neuronal differentiation and neurite outgrowth (Roux, Ballif, Anjum, Gygi, & Blenis, 2004). The survival of PC-12 cells is well documented to depend on activation of MAPK, which subsequently provides a canonical signaling cassette to promote neurogenesis, gene induction, and cell proliferation (Jordan, Landau, & Iyengar, 2000; Vaudry, Stork, Lazarovici, & Eiden, 2002). The present study advocates that, similar to the mechanism of action for NGF from snake venom or mouse submaxillary gland (Xing, Kornhauser, Xia, Thiele, & Greenberg, 1998), initiation of neurogenesis in PC-12 cells by Nn- α -elapitoxin-1 is largely dependent on activation of the MAPK signaling cascade.

Ligand-mediated activation of the TrkA receptor also triggers the activation of phospholipase C (PLC). The binding of NGF to the TrkA receptor elicits its cellular signaling by a complex network of intracellular proteins; TrkA receptor post-binding to NGF/ligands undergoes homodimerization and subsequent auto phosphorylation of its tyrosine residues (Cunningham, Stephens, Kaplan, & Greene, 1997; Segal et al., 1996). The activated TrkA receptor phosphorylates SHC, PI3K, and/or PLC γ 1 to act as the first-effector molecules, which in turn activate further signaling cascades, such as Ras/MAPK and Akt-pathways (Kaplan & Miller, 1997), which are well expressed in PC-12 cells post-treatment with Nn- α -elapitoxin-1 and mouse 2.5S-NGF. PLC γ supports activation of the protein kinase C (PKC) signaling pathway, which is involved in antimitogenic/mitogenic signaling pathway. Significant increase in the intracellular level of P-CREB proteins in Nn- α -elapitoxin-1-treated PC-12 cells evidently indicates activation of the above pathway.

Phosphorylation of the TrkA receptor results in membrane translocation of serine/threonine-protein kinases, leading to activation of Akt and p-Akt. This PI3K-Akt signaling pathway is extremely important for neuronal survival and the synthesis of many new cellular proteins for cell morphogenesis (Rahbek, Dissing, Thomassen, Hansen, & Tritsarlis, 2005). However, other researchers have presented contradictory findings showing that the PI3K-Akt pathway suppresses neurite branch formation in NGF-treated PC-12 cells (Higuchi, Onishi, Masuyama, & Gotoh, 2003). Up-regulation of the phosphorylated form of Akt in PC-12 cells post-treatment with Nn- α -elapitoxin-1 and partial inhibition of neurogenesis by chemical inhibitors of this pathway suggests that PI3K-Akt is a positive regulator of neurotrophin-induced neuronal differentiation in PC-12

cells, though this is a minor pathway for initiating neuritogenesis by Nn- α -elapitoxin-1. Based on the transcriptomics and proteomic analyses, it may be proposed that after ligand (Nn- α -elapitoxin-1)-TrkA binding, a second adaptor protein-growth factor-receptor bound protein-2 (Grb2) and a docking protein Grb2-associated binder-1 (GAB1) are activated which is followed by the activation of PI3K, which subsequently activates Akt kinase (Lad, Peterson, Bradshaw, & Neet, 2003; Song & Yoo, 2011).

Ligand-mediated activation of the TrkA receptor also triggers NF- κ B, which is a nuclear transcription factor regulating the expression of a large number of genes that are crucial for regulating cell survival (Brennan, Rivas-Plata, & Landis, 1999). The three-fold up-regulated expression of anti-apoptotic protein Bcl-2 in Nn- α -elapitoxin-1-treated PC-12 cells in a manner similar to that shown for mouse 2.5S-NGF indicates that Nn- α -elapitoxin-1 inhibits apoptosis to promote proliferation, differentiation, and neuronal survival (Kato, Mitsui, Kitani, & Suzuki, 1996). The suppressed expression of pro-apoptotic proteins such as P-JNK and BAX reinforces that Nn- α -elapitoxin-1 does not induce apoptosis in PC-12 cells (Dhanasekaran & Reddy, 2008). This is also supported by the lack of cell cytotoxicity and an inability to induce DNA fragmentation, hallmarks of apoptosis (Finegan, Wang, Lee, Robinson, & Tournier, 2009), by Nn- α -elapitoxin-1 in PC-12 cells.

The unique up-regulation of G alpha-15 protein (RAT|RGD=619751|UniProtKB=O88302) in chemokine and cytokine signaling pathways triggered by Nn- α -elapitoxin-1, are known to regulate diverse functions in the adult brain (Edman et al., 2008). This protein is also responsible for modulating the phospholipase C-activating dopamine receptor signaling pathway, where dopamine acts as a neurotransmitter and its correct balance is crucial for mental and physical wellbeing. Furthermore, the FGF-13 protein (RAT|RGD=620164|UniProtKB=Q9ERW3) from the FGF pathway is uniquely expressed in Nn- α -elapitoxin-1-treated PC-12 cells. This specific protein is of great importance as it participates in the refinement of axons by polymerization and stabilization of microtubules, thus playing a crucial role in polarization of neurons and their migration in the cerebral cortex and hippocampus (Ornitz & Itoh, 2015). In addition, neuron-associated disorders and apoptosis-related pathways have been found to be down-regulated by Nn- α -elapitoxin-1 which indicates that this Cobra venom toxin at nanomolar concentrations can assist in PC-12 cell survival and differentiation, a function that resembles that of mammalian NGF (Allen, Watson, Shoemark, Barua, & Patel, 2013). The expressions of above proteins are specific and unique to Nn- α -elapitoxin-1, which have not been demonstrated in mouse 2.5S-NGF-treated PC-12 cells.

5 | CONCLUSION

This is the first report to demonstrate the unique functional property of a long-chain neurotoxin (Nn- α -elapitoxin-1) from Indian cobra (*N. naja*) venom as a neurotrophin molecule. The receptor specificity and the high affinity binding of Nn- α -elapitoxin-1 to the TrkA receptor

initiates neuritogenesis without the co-activation of p⁷⁵NTR in the PC-12 cells. This is distinct from the mechanism of neuritogenesis induction by mammalian neurotrophins studied so far. Transcriptomics and proteomics studies have revealed that apart from activation of MAPK, there are common pathway for inducing neuritogenesis by both mouse 2.5S-NGF and Nn- α -elapitoxin-1; moreover, the latter molecule also influences other distinct signaling pathways for neuritogenesis which have not been demonstrated before.

ACKNOWLEDGEMENT

The authors thank C-CAMP, NCBS, Bangalore, for LC-MS/MS analysis. T.I. and M.M. received INSPIRE Senior Research Fellowships from DST, New Delhi. Some of the instrumental facilities used for this study were supported by grant from DBT, New Delhi, sponsored project (BT/410/NE/U-Excel/2013) to RM. This study received financial support from DBT, New Delhi (DBT/IC2/Indo-Russia/2014-16/03) and SERB, New Delhi (SERB/F/9755/2015-2019) sponsored projects to A.K.M.

All experiments were conducted in compliance with the ARRIVE guidelines.

CONFLICT OF INTEREST

The authors of this manuscript certify that they have No conflict of interest involved in any organization or entity or non-financial interest (such as personal or professional relationships, affiliations, knowledge, or beliefs) in the subject matter or materials discussed in this manuscript.

ORCID

Ashis K. Mukherjee  <https://orcid.org/0000-0001-9869-858X>

REFERENCE

- Alama, A., Bruzzo, C., Cavaliere, Z., Forlani, A., Utkin, Y., Casciano, I., & Romani, M. (2011). Inhibition of the nicotinic acetylcholine receptors by cobra venom α -neurotoxins: Is there a perspective in lung cancer treatment? *PLoS One*, 6, e20695. <https://doi.org/10.1371/journal.pone.0020695>
- Allen, S. J., Watson, J. J., Shoemark, D. K., Barua, N. U., & Patel, N. K. (2013). GDNF, NGF and BDNF as therapeutic options for neurodegeneration. *J Pharmacology Therapeutics*, 138, 155-175. <https://doi.org/10.1016/j.pharmthera.2013.01.004>
- Andrews, S. (2010). *FastQC: A quality control tool for high throughput sequence data*. Cambridge, UK: Babraham Bioinformatics, Babraham Institute.
- Ben-rong, H., & Ze, Z. (1995). Purification and characterization of a novel neurotoxin-kappa bungarotoxin. In L. C. Tang, & S. J. Tang (Eds.), *Neurochemistry in clinical application* (pp. 75-76). US, Boston, MA: Springer.
- Bibel, M., Hoppe, E., & Barde, Y. A. (1999). Biochemical and functional interactions between the neurotrophin receptors trk and p75NTR. *The EMBO Journal*, 18, 616-622. <https://doi.org/10.1093/emboj/18.3.616>
- Brennan, C., Rivas-Plata, K., & Landis, S. C. (1999). The p75 neurotrophin receptor influences NT-3 responsiveness of sympathetic neurons in vivo. *Nature Neuroscience*, 2, 699. <https://doi.org/10.1038/11158>
- Cargnello, M., & Roux, P. P. (2011). Activation and function of the MAPKs and their substrates, the MAPK-activated protein kinases.



- Microbiology and Molecular Biology Reviews*, 75, 50–83. <https://doi.org/10.1128/MMBR.00031-10>
- Chanda, A., Kalita, B., Patra, A., Senevirathne, W., & Mukherjee, A. K. (2018). Proteomic analysis and antivenomics study of Western India Naja naja venom: Correlation between venom composition and clinical manifestations of cobra bite in this region. *Expert Review of Proteomics*, 16(2), 171–184.
- Chanda, A., & Mukherjee, A. K. (2020). Quantitative proteomics to reveal the composition of Southern India spectacled cobra (*Naja naja*) venom and its immunological cross-reactivity towards commercial antivenom. *J International Journal of Biological Macromolecules*, 160, 224–232. <https://doi.org/10.1016/j.ijbiomac.2020.05.106>
- Chapeaurouge, A., Reza, M. A., Mackessy, S. P., Carvalho, P. C., Valente, R. H., Teixeira-Ferreira, A., ... Kini, R. M. (2015). Interrogating the venom of the Viperid Snake *Sistrurus catenatus edwardsii* by a combined approach of electrospray and MALDI mass spectrometry. *PLoS One*, 10, e0092091. <https://doi.org/10.1371/journal.pone.0092091>
- Chen, X.-Q., Sawa, M., & Mobley, W. C. (2017). Dysregulation of neurotrophin signaling in the pathogenesis of Alzheimer disease and of Alzheimer disease in Down syndrome. *Free Radical Biology and Medicine*, 114, 52–61. <https://doi.org/10.1016/j.freeradbiomed.2017.10.341>
- Chetty, R. (2019). Neurotrophic tropomyosin or tyrosine receptor kinase (NTRK) genes. *Journal of Clinical Pathology*, 72(3), 187–190.
- Cunningham, M. E., Stephens, R. M., Kaplan, D. R., & Greene, L. A. (1997). Autophosphorylation of activation loop tyrosines regulates signaling by the TRK nerve growth factor receptor. *The Journal of Biological Chemistry*, 272, 10957–10967. <https://doi.org/10.1074/jbc.272.16.10957>
- Darden, T., York, D., & Pedersen, L. (1993). Particle mesh Ewald: An N² log(N) method for Ewald sums in large systems. *The Journal of Chemical Physics*, 98, 10089–10092.
- Descamps, S., Pawlowski, V., Révillion, F., Hornez, L., Hebbar, M., Boilly, B., ... Peyrat, J.-P. (2001). Expression of nerve growth factor receptors and their prognostic value in human breast cancer. *J Cancer Research*, 61, 4337–4340.
- Dhanasekaran, D. N., & Reddy, E. P. (2008). JNK signaling in apoptosis. *Oncogene*, 27, 6245–6251. <https://doi.org/10.1038/onc.2008.301>
- Duhovny, D., Nussinov, R., & Wolfson, H. J. (2002). Efficient unbound docking of rigid molecules. In R. Guigó, & D. Gusfield (Eds.), *Algorithms in bioinformatics* (pp. 185–200). Berlin Heidelberg, Berlin, Heidelberg: Springer.
- Dutta, S., Chanda, A., Kalita, B., Islam, T., Patra, A., & Mukherjee, A. K. (2017). Proteomic analysis to unravel the complex venom proteome of eastern India *Naja naja*: Correlation of venom composition with its biochemical and pharmacological properties. *Journal of Proteomics*, 156, 29–39. <https://doi.org/10.1016/j.jpro.2016.12.018>
- Dutta, S., Gogoi, D., & Mukherjee, A. K. (2015). Anticoagulant mechanism and platelet deaggregation property of a non-cytotoxic, acidic phospholipase A2 purified from Indian cobra (*Naja naja*) venom: Inhibition of anticoagulant activity by low molecular weight heparin. *Biochimie*, 110, 93–106. <https://doi.org/10.1016/j.biochi.2014.12.020>
- Dutta, S., Sinha, A., Dasgupta, S., & Mukherjee, A. K. (2019). Binding of a *Naja naja* venom acidic phospholipase A2 cognate complex to membrane-bound vimentin of rat L6 cells: Implications in cobra venom-induced cytotoxicity. *Biochimica Et Biophysica Acta (BBA) - Biomembranes*, 1861, 958–977. <https://doi.org/10.1016/j.bbmem.2019.02.002>
- Edman, L. C., Mira, H., & Arenas, E. (2008). The beta-chemokines CCL2 and CCL7 are two novel differentiation factors for midbrain dopaminergic precursors and neurons. *Experimental Cell Research*, 314, 2123–2130.
- Eggert, A., Sieverts, H., Ikegaki, N., & Brodeur, G. M. (2000). p75 mediated apoptosis in neuroblastoma cells is inhibited by expression of TrkA. *Medical and Pediatric Oncology: The Official Journal of SIOP—International Society of Pediatric Oncology (Société Internationale D'oncologie Pédiatrique)*, 35, 573–576. [https://doi.org/10.1002/1096-911X\(20001201\)35:6<573:AID-MPO17>3.0.CO;2-A](https://doi.org/10.1002/1096-911X(20001201)35:6<573:AID-MPO17>3.0.CO;2-A)
- Finegan, K. G., Wang, X., Lee, E.-J., Robinson, A. C., & Tournier, C. (2009). Regulation of neuronal survival by the extracellular signal-regulated protein kinase 5. *Cell Death and Differentiation*, 16, 674. <https://doi.org/10.1038/cdd.2008.193>
- Guex, N., & Peitsch, M. C. (1997). SWISS-MODEL and the Swiss-PdbViewer: An environment for comparative protein modeling. *Electrophoresis*, 18, 2714–2723. <https://doi.org/10.1002/elps.1150181505>
- Harrington, A. W., & Ginty, D. D. (2013). Long-distance retrograde neurotrophic factor signalling in neurons. *Nature Reviews Neuroscience*, 14, 177–187. <https://doi.org/10.1038/nrn3253>
- Hempstead, B. L. (2006). Dissecting the diverse actions of pro- and mature neurotrophins. *Current Alzheimer Research*, 3, 19–24.
- Hess, B. (2008). P-LINCS: A parallel linear constraint solver for molecular simulation. *Journal of Chemical Theory and Computation*, 4, 116–122.
- Hess, B., Bekker, H., Berendsen, H. J., & Fraaije, J. G. (1997). LINCS: A linear constraint solver for molecular simulations. *Journal of Computational Chemistry*, 18, 1463–1472. [https://doi.org/10.1002/\(SICI\)1096-987X\(199709\)18:12<1463:AID-JCC4>3.0.CO;2-H](https://doi.org/10.1002/(SICI)1096-987X(199709)18:12<1463:AID-JCC4>3.0.CO;2-H)
- Higuchi, M., Onishi, K., Masuyama, N., & Gotoh, Y. (2003). The phosphatidylinositol-3 kinase (PI3K)-Akt pathway suppresses neurite branch formation in NGF-treated PC12 cells. *Genes to Cells: Devoted to Molecular and Cellular Mechanisms*, 8, 657–669. <https://doi.org/10.1046/j.1365-2443.2003.00663.x>
- Höpker, V. H., Saffrey, M. J., & Burnstock, G. (1996). Neurite outgrowth of striatal neurons in vitro: Involvement of purines in the growth-promoting effect of myenteric plexus explants. *International Journal of Developmental Neuroscience*, 14, 439–451.
- Huang, E. J., & Reichardt, L. F. (2001). Neurotrophins: Roles in neuronal development and function. *Annual Review of Neuroscience*, 24, 677–736. <https://doi.org/10.1146/annurev.neuro.24.1.677>
- Isom, G. E., & Borowitz, J. (2016). PC-12 Cells. In *Vitro Biological Systems: Methods in Toxicology* 1.
- Joca, S. R., Moreira, F. A., & Wegener, G. (2015). Atypical neurotransmitters and the neurobiology of depression. *CNS and Neurological Disorders Drug Targets*, 14, 1001–1011.
- Jordan, J. D., Landau, E. M., & Iyengar, R. (2000). Signaling networks: The origins of cellular multitasking. *Cell*, 103, 193–200. [https://doi.org/10.1016/S0092-8674\(00\)00112-4](https://doi.org/10.1016/S0092-8674(00)00112-4)
- Kalita, B., Patra, A., Das, A., & Mukherjee, A. K. (2018). Proteomic analysis and immuno-profiling of eastern India Russell's Viper (*Daboia russelii*) venom: Correlation between RVV composition and clinical manifestations post RV bite. *Biochimica Et Biophysica Acta (BBA) - Biomembranes*, 17, 2819–2833.
- Kalita, B., Patra, A., & Mukherjee, A. K. (2017). unraveling the proteome composition and immuno-profiling of western india russell's viper venom for in-depth understanding of its pharmacological properties, clinical manifestations, and effective antivenom treatment. *Journal of Proteome Research*, 16, 583–598. <https://doi.org/10.1021/acs.jproteome.6b00693>
- Kaplan, D. R., & Miller, F. D. (1997). Signal transduction by the neurotrophin receptors. *Current Opinion in Cell Biology*, 9, 213–221.
- Kapranov, P., Willingham, A. T., & Gingeras, T. R. (2007). Genome-wide transcription and the implications for genomic organization. *Nature Reviews Genetics*, 8, 413–423. <https://doi.org/10.1038/nrg2083>
- Katoh, S., Mitsui, Y., Kitani, K., & Suzuki, T. (1996). Nerve growth factor rescues PC12 cells from apoptosis by increasing amount of bcl-2. *Biochemical and Biophysical Research Communications*, 229, 653–657. <https://doi.org/10.1006/bbrc.1996.1859>
- Katz, M., Amit, I., & Yarden, Y. (2007). Regulation of MAPKs by growth factors and receptor tyrosine kinases. *Biochimica Et Biophysica Acta*

- (BBA) - *Biomembranes*, 1773, 1161–1176. <https://doi.org/10.1016/j.bbamcr.2007.01.002>
- Kim, D., Langmead, B., & Salzberg, S. L. (2015). HISAT: A fast spliced aligner with low memory requirements. *Nature Methods*, 12, 357. <https://doi.org/10.1038/nmeth.3317>
- Krueger, F. (2015). A wrapper tool around Cutadapt and FastQC to consistently apply quality and adapter trimming to FastQ files, 516, 517. http://www.bioinformatics.babraham.ac.uk/projects/trim_galore/
- Kruger, D. M., & Gohlke, H. (2010). DrugScorePPI webserver: Fast and accurate in silico alanine scanning for scoring protein-protein interactions. *Nucleic Acids Research*, 38, W480–486. <https://doi.org/10.1093/nar/gkq471>
- Kuo, K.-W., Chang, L.-S., & Chang, C.-C. (1995). The structural loop II of cobrotoxin is the main binding region for nAChR and epitope in the region is conformation-dependent. *The Journal of Biochemistry*, 117, 438–442. <https://doi.org/10.1093/jb/117.2.438>
- Lad, C., Williams, N. H., & Wolfenden, R. (2003). The rate of hydrolysis of phosphomonoester dianions and the exceptional catalytic proficiencies of protein and inositol phosphatases. *Proceedings of the National Academy of Sciences*, 100, 5607–5610. <https://doi.org/10.1073/pnas.0631607100>
- Lad, S. P., Peterson, D. A., Bradshaw, R. A., & Neet, K. E. (2003). Individual and combined effects of TrkA and p75NTR nerve growth factor receptors. A role for the high affinity receptor site. *The Journal of Biological Chemistry*, 278, 24808–24817.
- Laskowski, R. A. (2001). PDBsum: Summaries and analyses of PDB structures. *Nucleic Acids Research*, 29, 221–222. <https://doi.org/10.1093/nar/29.1.221>
- Li, H., Handsaker, B., Wysoker, A., Fennell, T., Ruan, J., Homer, N., ... Durbin, R. J. B. (2009). The sequence Alignment/Map format and SAMtools. *Bioinformatics*, 25, 2078–2079. <https://doi.org/10.1093/bioinformatics/btp352>
- Li, Q. J., Yang, S. H., Maeda, Y., Sladek, F. M., Sharrocks, A. D., & Martins-Green, M. (2003). MAP kinase phosphorylation-dependent activation of Elk-1 leads to activation of the co-activator p300. *The EMBO Journal*, 22, 281–291. <https://doi.org/10.1093/emboj/cdg028>
- Li, X., Keskin, O., Ma, B., Nussinov, R., & Liang, J. (2004). Protein-protein interactions: Hot spots and structurally conserved residues often locate in complemented pockets that pre-organized in the unbound states: Implications for docking. *Journal of Molecular Biology*, 344, 781–795. <https://doi.org/10.1016/j.jmb.2004.09.051>
- Loers, G., Chen, S., Grumet, M., & Schachner, M. (2005). Signal transduction pathways implicated in neural recognition molecule L1 triggered neuroprotection and neuritogenesis. *Journal of Neurochemistry*, 92, 1463–1476. <https://doi.org/10.1111/j.1471-4159.2004.02983.x>
- Longo, F. M., & Massa, S. M. (2013). Small-molecule modulation of neurotrophin receptors: A strategy for the treatment of neurological disease. *Nature Reviews Drug Discovery*, 12, 507. <https://doi.org/10.1038/nrd4024>
- Lowry, O. H., Rosebrough, N. J., Farr, A. L., & Randall, R. J. (1951). Protein measurement with the Folin phenol reagent. *J Journal of Biological Chemistry*, 193, 265–275.
- Lyukmanova, E. N., Shenkarev, Z. O., Shulepko, M. A. et al (2015). Structural insight into specificity of interactions between nonconventional three-finger weak toxin from *Naja kaouthia* (WTX) and muscarinic acetylcholine receptors. *Journal of Biological Chemistry*, 290, 23616–23630.
- Marshall, C. (1995). Specificity of receptor tyrosine kinase signaling: Transient versus sustained extracellular signal-regulated kinase activation. *Cell*, 80, 179–185. [https://doi.org/10.1016/0092-8674\(95\)90401-8](https://doi.org/10.1016/0092-8674(95)90401-8)
- Massa, S. M., Yang, T., Xie, Y., Shi, J., Bilgen, M., Joyce, J. N., ... Longo, F. M. (2010). Small molecule BDNF mimetics activate TrkB signaling and prevent neuronal degeneration in rodents. *The Journal of Clinical Investigation*, 120, 1774–1785. <https://doi.org/10.1172/JCI41356>
- Melan, M. A., & Sluder, G. (1992). Redistribution and differential extraction of soluble proteins in permeabilized cultured cells. Implications for immunofluorescence microscopy. *Journal of Cell Science*, 101, 731–743.
- Mohan, S. K., & Yu, C. (2007). Structure function relationships of Cobrotoxin from *Naja naja atra*. *Toxin Reviews*, 26, 99–122.
- Mukherjee, A. K., Kalita, B., & Mackessy, S. P. (2016). A proteomic analysis of Pakistan *Daboia russelii russelii* venom and assessment of potency of Indian polyvalent and monovalent antivenom. *Journal of Proteomics*, 144, 73–86. <https://doi.org/10.1016/j.jprot.2016.06.001>
- Mukherjee, A. K., & Mackessy, S. P. (2014). Pharmacological properties and pathophysiological significance of a Kunitz-type protease inhibitor (Rusvikunin-II) and its protein complex (Rusvikunin complex) purified from *Daboia russelii russelii* venom. *Toxicon: Official Journal of the International Society on Toxicology*, 89, 55–66. <https://doi.org/10.1016/j.toxicon.2014.06.016>
- Nirathanan, S., & Gwee, M. C. (2004). Three-finger α -neurotoxins and the nicotinic acetylcholine receptor, forty years on. *Journal of Pharmacological Sciences*, 94, 1–17. <https://doi.org/10.1254/jphs.94.1>
- Ofran, Y., & Rost, B. (2003). Analysing six types of protein-protein interfaces. *Journal of Molecular Biology*, 325, 377–387. [https://doi.org/10.1016/S0022-2836\(02\)01223-8](https://doi.org/10.1016/S0022-2836(02)01223-8)
- Ornitz, D. M., & Itoh, N. (2015). The fibroblast growth factor signaling pathway. *Wiley Interdisciplinary Reviews: Developmental Biology*, 4, 215–266. <https://doi.org/10.1002/wdev.176>
- Park, H., & Poo, M.-M. (2012). Neurotrophin regulation of neural circuit development and function. *Nature Reviews Neuroscience*, 14, 7. <https://doi.org/10.1038/nrn3379>
- Parrinello, M., & Rahman, A. (1980). Crystal structure and pair potentials: A molecular-dynamics study. *Physical Review Letters*, 45, 1196. <https://doi.org/10.1103/PhysRevLett.45.1196>
- Patapoutian, A., & Reichardt, L. F. (2001). Trk receptors: Mediators of neurotrophin action. *Current Opinion in Neurobiology*, 11, 272–280. [https://doi.org/10.1016/S0959-4388\(00\)00208-7](https://doi.org/10.1016/S0959-4388(00)00208-7)
- Patra, A., Kalita, B., Chanda, A., & Mukherjee, A. K. (2017). Proteomics and antivenomics of *Echis carinatus carinatus* venom: Correlation with pharmacological properties and pathophysiology of envenomation. *Scientific Reports*, 7, 17119. <https://doi.org/10.1038/s41598-017-17227-y>
- Perera, P., Bazaka, O., Bazaka, K., Appadoo, D., Croft, R., Crawford, R., & Ivanova, E. (2019). Pheochromocytoma (PC 12) as a model cell line for membrane permeabilization studies in the presence of electromagnetic fields (EMFs): Recent advances. *Journal of Neurology and Neuromedicine*, 4, 35–40.
- Pertea, M., Kim, D., Pertea, G. M., Leek, J. T., & Salzberg, S. L. (2016). Transcript-level expression analysis of RNA-seq experiments with HISAT, StringTie and Ballgown. *Nature Protocols*, 11(9), 1650–1667. <https://doi.org/10.1038/nprot.2016.095>
- Pertea, M., Pertea, G. M., Antonescu, C. M., Chang, T.-C., Mendell, J. T., Salzberg, S. L. (2015). StringTie enables improved reconstruction of a transcriptome from RNA-seq reads. *Nature Biotechnology*, 33(3), 290–295. <https://doi.org/10.1038/nbt.3122>
- Rahbek, U. L., Dissing, S., Thomassen, C., Hansen, A. J., & Tritsarlis, K. (2005). Nerve growth factor activates aorta endothelial cells causing PI3K/Akt-and ERK-dependent migration. *Pflügers Archiv - European Journal of Physiology*, 450, 355–361. <https://doi.org/10.1007/s00424-005-1436-0>
- Riss, T. L., Moravec, R. A., Niles, A. L., Duellman, S., Benink, H. A., Worzella, T. J., & Minor, L. (2016). Cell viability assays. *Assay Guidance Manual* [Internet]. Eli Lilly & Company and the National Center for Advancing Translational Sciences.
- Roux, P. P., Ballif, B. A., Anjum, R., Gygi, S. P., & Blenis, J. (2004). Tumor-promoting phorbol esters and activated Ras inactivate the tuberous sclerosis tumor suppressor complex via p90 ribosomal S6 kinase. *Proceedings of the National Academy of Sciences*, 101, 13489–13494. <https://doi.org/10.1073/pnas.0405659101>



- Rubenstein, R., Carp, R. I., & Callahan, S. M. (1984). In vitro replication of scrapie agent in a neuronal model: Infection of PC12 cells. *Journal of General Virology*, 65, 2191–2198. <https://doi.org/10.1099/0022-1317-65-12-2191>
- Schwede, T., Kopp, J., Guex, N., & Peitsch, M. C. (2003). SWISS-MODEL: An automated protein homology-modeling server. *Nucleic Acids Research*, 31, 3381–3385. <https://doi.org/10.1093/nar/gkg520>
- Segal, R. A., Bhattacharyya, A., Rua, L. A., Alberta, J. A., Stephens, R. M., Kaplan, D. R., & Stiles, C. D. (1996). Differential utilization of Trk autophosphorylation sites. *The Journal of Biological Chemistry*, 271, 20175–20181. <https://doi.org/10.1074/jbc.271.33.20175>
- Sintiprungrat, K., Watcharatanyatip, K., Senevirathne, W., Chaisuriya, P., Chokchaichamnankit, D., Srisomsap, C., & Ratanabanangkoon, K. (2016). A comparative study of venomomics of *Naja naja* from India and Sri Lanka, clinical manifestations and antivenomics of an Indian poly-specific antivenom. *Journal of Proteomics*, 132, 131–143. <https://doi.org/10.1016/j.jprot.2015.10.007>
- Song, E.-J., & Yoo, Y.-S. (2011). Nerve growth factor-induced neurite outgrowth is potentiated by stabilization of TrkA receptors. *BMB Reports*, 44, 182–186. <https://doi.org/10.5483/BMBRep.2011.44.3.182>
- Suryamohan, K., Krishnankutty, S. P., Guillory, J., Jevit, M., Schröder, M. S., Wu, M., ... Seshagiri, S. (2020). The Indian cobra reference genome and transcriptome enables comprehensive identification of venom toxins. *Nature Genetics*, 52(1), 106–117. <https://doi.org/10.1038/s41588-019-0559-8>
- Toni, T., Dua, P., & van der Graaf, P. H. (2014). Systems Pharmacology of the NGF Signaling Through p75 and TrkA Receptors. *CPT Pharmacometrics and Systems Pharmacology*, 3, e150. <https://doi.org/10.1038/psp.2014.48>
- Trummal, K., Tonismagi, K., Paalme, V., Jarvekulg, L., Siigur, J., & Siigur, E. (2011). Molecular diversity of snake venom nerve growth factors. *Toxicon: Official Journal of the International Society on Toxinology*, 58, 363–368. <https://doi.org/10.1016/j.toxicon.2011.07.005>
- Tuch, B. B., Laborde, R. R., Xu, X., Gu, J., Chung, C. B., Monighetti, C. K., ... Smith, D. I. (2010). Tumor transcriptome sequencing reveals allelic expression imbalances associated with copy number alterations. *PLoS One*, 5, e9317. <https://doi.org/10.1371/journal.pone.0009317>
- Vaudry, D., Stork, P. J. S., Lazarovici, P., & Eiden, L. E. (2002). Signaling pathways for PC12 cell differentiation: Making the right connections. *Science*, 296, 1648. <https://doi.org/10.1126/science.1071552>
- Wang, C. I., Reeks, T., Vetter, I., Vergara, I., Kovtun, O., Lewis, R. J., ... Durek, T. (2014). Isolation and structural and pharmacological characterization of alpha-elapitoxin-Dpp2d, an amidated three finger toxin from black mamba venom. *Biochemistry*, 53, 3758–3766.
- Wiederstein, M., & Sippl, M. J. (2007). ProSA-web: Interactive web service for the recognition of errors in three-dimensional structures of proteins. *Nucleic Acids Research*, 35, W407–410. <https://doi.org/10.1093/nar/gkm290>
- Xing, J., Kornhauser, J. M., Xia, Z., Thiele, E. A., & Greenberg, M. E. (1998). Nerve growth factor activates extracellular signal-regulated kinase and p38 mitogen-activated protein kinase pathways to stimulate CREB serine 133 phosphorylation. *Molecular and Cellular Biology*, 18, 1946–1955. <https://doi.org/10.1128/MCB.18.4.1946>
- Zhang C., Vasmataz G., Cornette J. L., & DeLisi C. (1997). Determination of atomic desolvation energies from the structures of crystallized proteins 1 Edited by B. Honig. *Journal of Molecular Biology*, 267, 707–726. <http://dx.doi.org/10.1006/jmbi.1996.0859>
- Zhang, Y.-Z., Moheban, D. B., Conway, B. R., Bhattacharyya, A., & Segal, R. A. (2000). Cell surface Trk receptors mediate NGF-induced survival while internalized receptors regulate NGF-induced differentiation. *Journal of Neuroscience*, 20, 5671–5678. <https://doi.org/10.1523/JNEUROSCI.20-15-05671.2000>

SUPPORTING INFORMATION

Additional supporting information may be found online in the Supporting Information section.

How to cite this article: Islam T, Majumder M, Kalita B, Bhattacharjee A, Mukhopadhyay R, Mukherjee AK. Transcriptomic, proteomic, and biochemical analyses reveal a novel neuritogenesis mechanism of *Naja naja* venom α -elapitoxin post binding to TrkA receptor of rat pheochromocytoma cells. *J. Neurochem.* 2020;155:612–637. <https://doi.org/10.1111/jnc.15153>